Design, synthesis and testing of calpain inhibitors for the treatment of cataract

A thesis submitted in partial fulfillment of the requirements of the degree of

Master of Science in Chemistry

University of Canterbury

by

Hongyuan Chen

2007

TABLE OF CONTENTS

ABSTRACT

This thesis reports the development of potent and selective inhibitors of m-calpain for the treatment of cataract.

SJA6017 has been proven to prevent lens opacity in rat and has been our lead compound. A series of Val-Leu peptidyl aldehyde inhibitors (**33a-e, 33g, 33i** and **35)** have been designed, synthesized, and tested for therapeutic potential as cataract inhibitors.

Chapter 1 is an introduction to calpain and the diseases associated with it's over activation. A review of the literature on calpain inhibition is given. Structure activity relationship (SAR) theory is presented. The techniques that have been applied in our research group to drug design include molecular modeling, synthesis, assay and animal studies which are all briefly discussed. The importance of a β-strand conformation for an inhibitor to bind to calpain is discussed.

Chapter 2 describes the synthesis of m-calpain inhibitors. This comprises the preparation of the Val-Leu dipeptide core **29**, Val-Leu dipeptidyl alcohols **31a-g** and **31i**, and the synthesis of dipeptidyl aldehydes **33a-e, 33g, 33i** and **35**. The choice of coupling regents and conditions in the coupling reactions is investigated. Sulfur trioxide pyridine oxidation for the conversion of Val-Leu dipeptidyl alcohols to aldehydes is discussed. The molecular modeling and biological assay results are presented.

ABBREVIATIONS

BOC	tert-butoxycarbonyl
d	doublet (in NMR)
^{13}C NMR	carbon nuclear magnetic resonance
Cys	cysteine
DCM	dichloromethane
DIPEA	diisopropylethylamine
DMAP	4-(dimethylamino)pyridine
DMF	N,N-dimethylformamide
DMSO	dimethyl sulfoxide
EDC	1-[3-(dimethylamino)propyl]-3-ethylcarbodiimide hydrochloride
EtOAc	ethyl acetate
HATU	O-(7-azabenzotriazol-1-yl)-1,1,3,3-tetramethyluronium hexafluorophosphate
HBTU	O-(benzotriazol-1-yl)-1,1,3,3-tetramethyluronium hexafluorophosphate
His	histidine
HOAt	1-hydroxy-7-azabenzotriazole
HOBt	1-hydroxybenzotriazole
^{1}H-NMR	proton nuclear magnetic resonance
Hz	Hertz (in NMR)
IC_{50}	inhibitor concentration that decrease enzyme activity by 50%
Leu	leucine
m	multiplet (in NMR)
MeOH	methanol
min	minutes
mp	melting point
MS	mass spectrometry
NMR	nuclear magnetic resonance
ppm	parts per million
RCM	ring closing metathesis
s	singlet (in NMR)
SAR	structure and activity relationship
SO_3.Pyr	sulphur trioxide-pyridine complex
t	triplet (in NMR)
THF	tetrahydrofuran
TLC	thin-layer chromatography
UV	ultraviolet
Val	valine

ACKNOWLEGEMENT

Firstly, I would like to say thank you to my supervisors, Professors Jim Coxon and Andrew Abell. I remain grateful for being accepted into the calpain research group and for the opportunity provided.

Thank you to my wonderful group members for their friendship and support. I would like to thank the following people for their help: Hayden Peacock and Seth Jones for their laboratory assistance, Janna Nikkel for assays, Wanting Jiao for computer modeling, Rewi Thompson and Gill Ellis for NMR, Robert Stainthorpe for the mass spectrometry and finally Dr Matthew Jones. Matt has been an excellent instructor. Without his guidance, encouragement, and support, my work would have been less fruitful.

Thank you my parents for believing in me and showing their support throughout my graduate study.

Chapter 1: Introduction

1.1: Calpain Structure

Proteases are the enzymes that catalyze the cleavage of target proteins into smaller peptide fragments and amino acids. Peptide hydrolysis depends on key catalytic residues and as such proteases have been classified into serine, threonine, cysteine, aspartic acid, metallo, and glutamic acid proteases.

Molecular biological studies have shown that calpains are calcium-dependent cysteine proteases. There are two major calpain isoforms, known as calpain I (μ-calpain) and calpain II (m-calpain). They have the same substrate specificity and both subunits contain multiple Ca^{2+} binding EF-hands. They differ in the Ca^{2+} concentration requirement for activation.[1] Calpain I requires a micromolar concentration of Ca^{2+} (1-100 μM) whereas calpain II is activated by millimolar concentration of Ca^{2+} (0.1-1 mM).[2]

Calpain contains a large catalytic subunit (80-kDa) and a small regulatory subunit (30-kD). The typical large subunit of calpain is composed of four domains (I–IV) and the small subunit of calpain has at least two domains (V and VI). Ca^{2+} binds at the sites of two calmodulin-like domains IV and VI, an acidic loop region in domain III, and the protease domain II (**Figure 1**). Ca^{2+} binding releases the constraints imposed by domain interactions, and rearranges the active site cleft to form a functional catalytic site.[3]

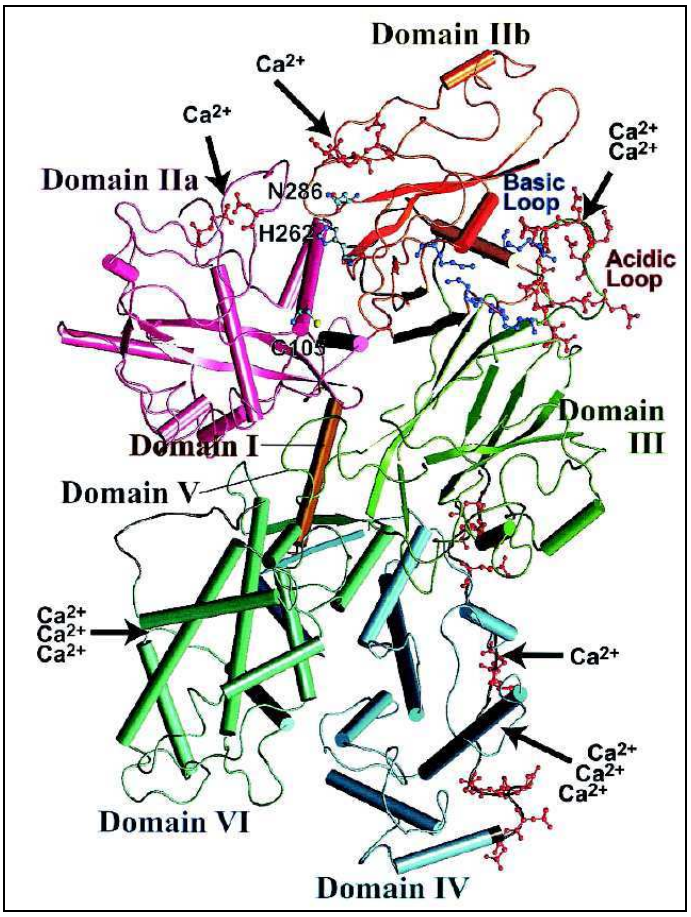

Figure 1: Three-dimensional structure of human m-calpain without Ca^{2+} bound.[4]

Recent X-ray structures of mini μ- and m-calpain constructs has revealed the Ca^{2+}-induced activation mechanism at the molecular level.[5] A crystal structure of human m-calpain in an un-activated form was obtained (**Figure 2A**). This structure revealed that without calcium bound the distance between sulfur of Cys_{105} and the imidazole nitrogen of His_{262} of the catalytic triad is 8.5 Å. It was not possible to get an X-ray crystal structure of an activated calpain, as calpain is autolytic, therefore site directed mutagenesis was used to convert Cys_{115} to Ser_{115}. The crystal structure of a calcium bound mini μ-calpain mutant construct revealed the distance between oxygen of Ser_{115}

and the imidazole nitrogen of His_{272} is 3.7 Å (**Figure 2B**). This conformational change of the catalytic triad "cysteine-histidine-asparagine" leads to activated calpain which can catalyze the cleavage of amide linkages in calpain substrates.

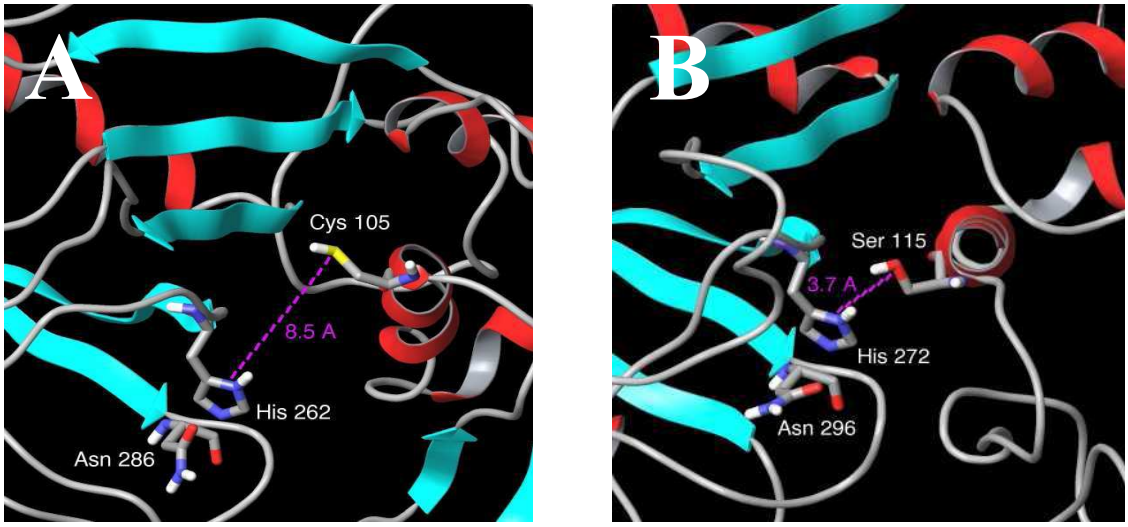

Figure 2: X-ray crystal structures of A) An un-activated m-calpain construct. B) An activated μ-calpain (Cys_{115} to Ser_{115}) construct.

To catalyze the hydrolysis of the peptide bonds, calpain firstly acts as a surface that binds the substrate to the active site. Calpain subsites bind the peptide chain on either side of the scissile peptide bond and show specificity for particular side chains.[3] The binding between the enzyme and substrate is determined by the electrostatic character and the size of the enzyme subsites. Binding of a substrate is designated using the standard nomenclature developed by Berger and Schechter (**Figure 3**).[6]

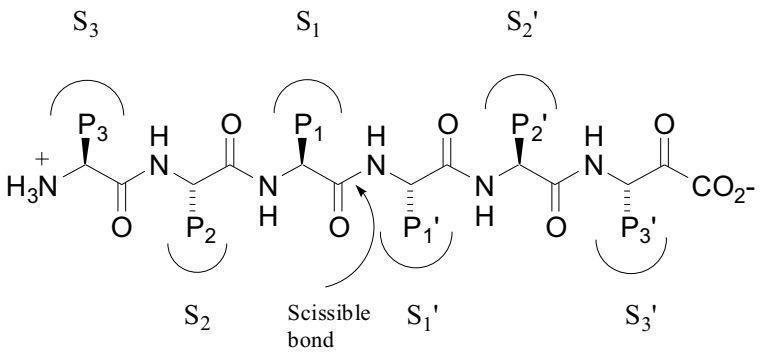

Figure 3: Amino acid residues and subsites from enzyme are denoted by P_1, P_2 and the S_1, S_2 etc towards the amino side of peptide from catalytic site. The carboxyl side of the peptide and corresponding subsites are termed P_1', P_2', Pn' and S_1', S_2'and Sn', respectively.

1.2: Mechanism of calpain activation

The crystal structure of m-calpain without calcium bound is illustrated and the active site (domain II) and Ca^{2+} bonding sites (domains IV, VI) are shown in **Figure 1**. Conformations of the catalytic triad in active and inactive states of calpain are shown in **Figure 2**. The conformational change on bonding of calcium lowers the activation energy for the substrate hydrolysis and the structure-based mechanism has been thereby proposed.[7]

To catalyze the hydrolysis of peptide bonds, the first step is deprotonation of a thiol in the active site of calpain by a histidine residue of an adjacent amino acid. The next step is nucleophilic attack by the activated cysteine's anionic sulfur on the substrate carbonyl carbon to form thioester intermediate. A fragment of the substrate is released having an amine terminus. The thioester bond is hydrolyzed to generate a carboxylic acid and

regenerates the free enzyme (**Scheme 1**).

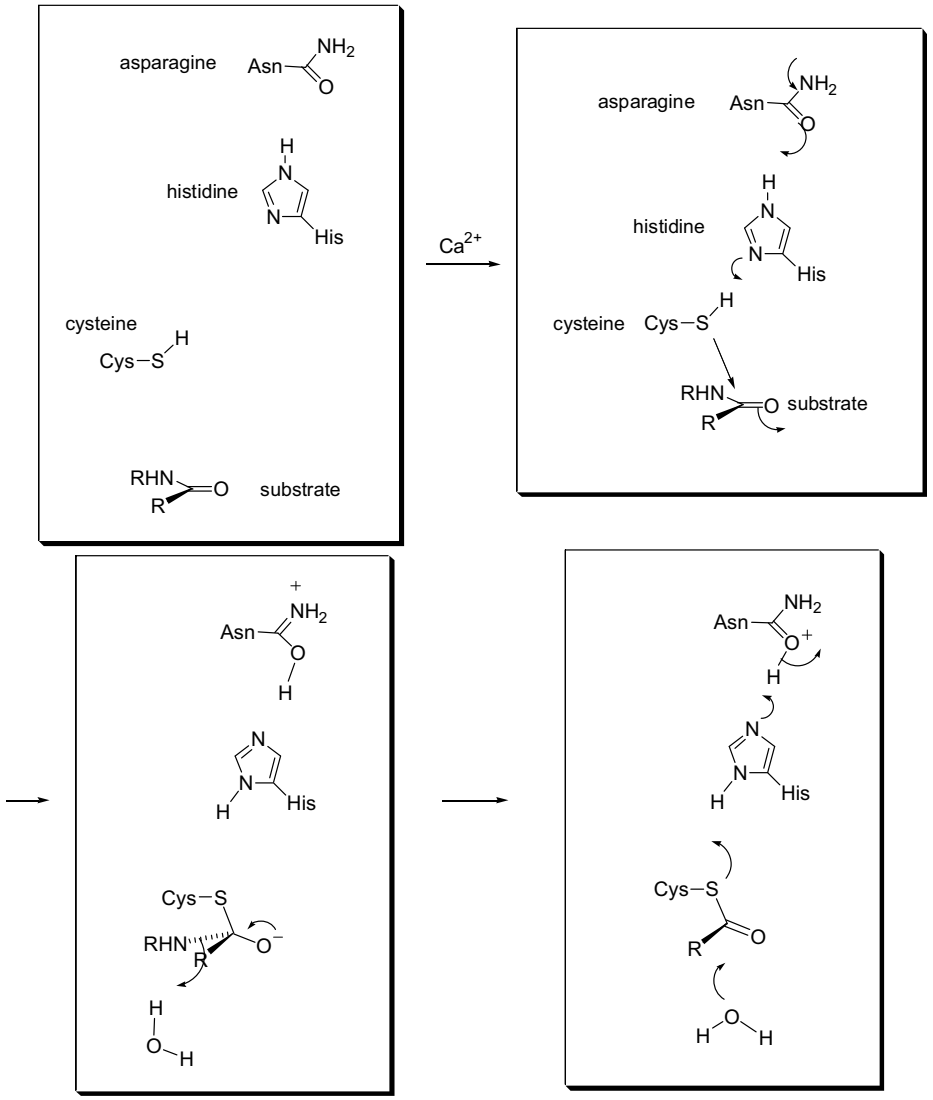

Scheme 1: The mechanism of action of cysteine proteases.

Calpains can cleave a large number of substrates and show specificity for bonding of the amino acid neighboring the cleavage site. Cleavage occurs frequently at the C-terminal side (P_1 position) of tyrosine, methionine, or arginine, next to leucine or valine (P_2 position).[8]

1.3: Calpain and Disease

The overactivation of calpain has been observed in several medicine conditions such as Alzheimer's,[9,10] Huntington's, Parkinson's diseases,[11] ischemic and traumatic brain injury,[12] cancer, Muscular Dystrophy, strokes, diabetes and cataract.[13] (**Table 1**)

Calpain	Diseases
Calpain 1	stroke, traumatic brain injury, Alzheimer's disease, cataracts
Calpain 2	stroke, traumatic brain injury, Alzheimer's disease, cataracts
Calpain 3	Limb-girdle muscular dystrophy 2A, cataracts
Calpain 9	gastric cancer
Calpain 8/10	Type 2 diabetes mellitus

Table 1: Calpain family and various pathological conditions.[14]

The over activation of calpain I can cleave and activate calcineurin. Calcineurin (CaN) is known as protein phosphatase (PP)2B. The phosphatase activity of CaN is regulated by Ca^{2+}/calmodulin and calpain activation. The activation of calcineurin is related to the number of neurofibrillary tangles in human brains and hence mediates the role of calcium homeostatic disturbance in the neurodegeneration of Alzheimer's disease.[15]

Huntington's disease has also been correlated with the calpain activity. The activated calpain catalyzes the hydrolysis of the Huntington protein at multiple sites and the resulting toxic protein fragments are responsible for neuronal loss leading to Huntington's disease.[16]

A substrate for calpain called α-synuclein is the major component of lewy bodies (LBs). LBs are hallmark lesions of degenerating neurons in the brains which can lead to Parkinson's disease (PD).[17]

Loss-of-function mutations of the calpain 3 gene have been identified as the cause of limb-girdle muscular dystrophy 2A.

Elevated calpain 5 levels have been correlated with polycystic ovary syndrome (PCOS), obesity, hypertension and dyslipidemia.[18]

1.4: Origin of cataract and its treatment

The lens of the human eye is located in the anterior segment and is a highly specialized non-vascular tissue. The lens focuses an image onto the retina of the eye, converting light energy into an electrical impulse. The impulses are then interpreted by the brain as vision (**Figure 4)**. Cataract is a disease of the eye that results in the lens becoming opaque and thereby distorting light as it passes through the lens. The opacification of the lens prevent the light from reaching the retina resulting in a decrease in the quality of vision and ultimately in blindness.

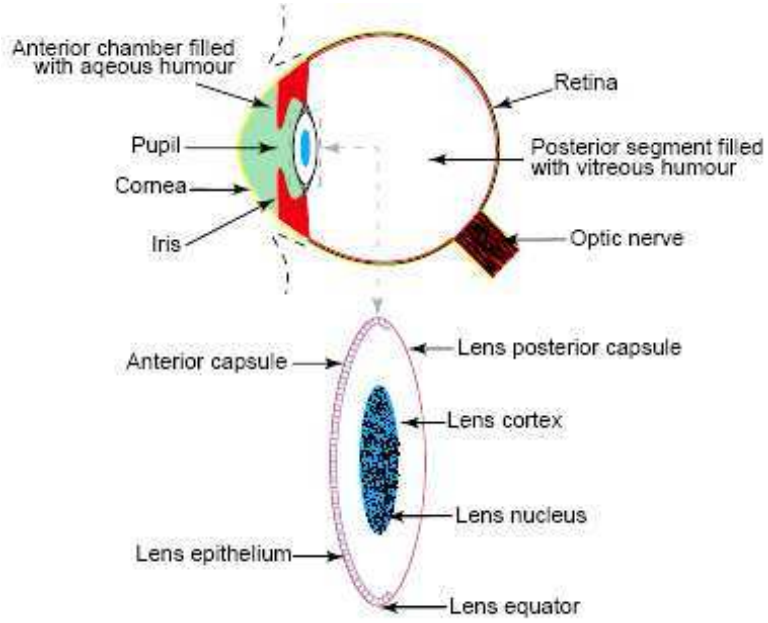

Figure 4: The way the human eye works.[19]

Cataract formation results from a variety of insults such as genotype, selenite and damage from ultraviolet light. Research on selected age cohorts of normal human subjects has shown that, on average, as the human lens ages, the intensity of light scattered backwards out of the pupil increases exponentially with age.[20]

The ageing process or other insults lead to impaired membrane function, which results in elevated levels of Ca^{2+} in the lens tissue. Under these conditions, calpains are overactivated and the resulting deregulated proteolysis of soluble crystallins leads to their insolubilization and aggregation. This compromises the function of crystallins in maintaining lens transparency and produces the reduced lens performance associated with cataract (**Figure 5**).[21] Thus, calpain activity is important and the development of calpain inhibitors could interfere with cataract progression.

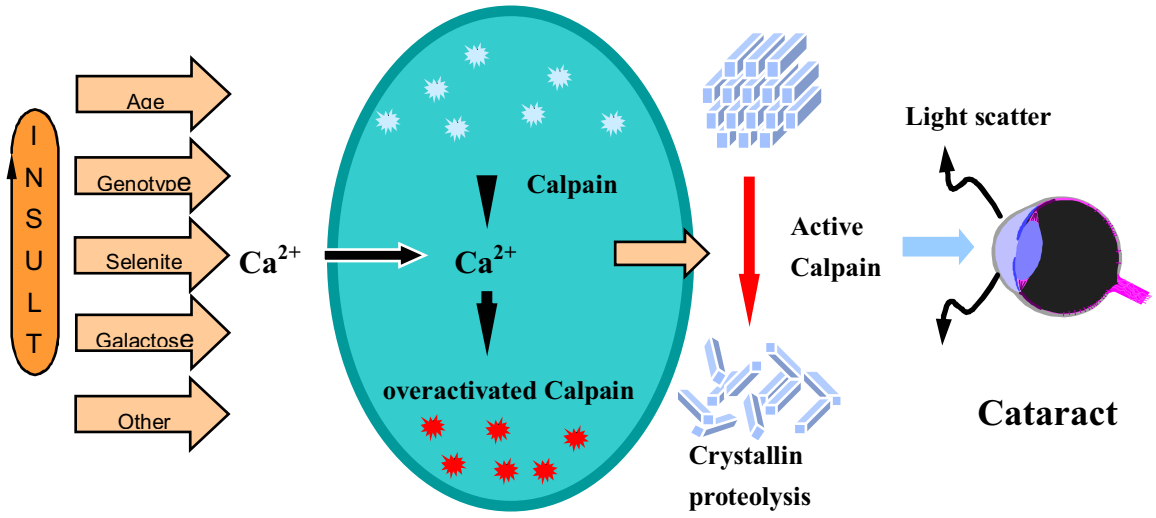

Figure 5: Calpain dependent cataract.[22]

Currently the only treatment for cataract is surgery. The lens of the eye that has developed a cataract is removed and replaced with an artificial intraocular lens.[23] This is a safe and successful procedure for cataract treatment. However, the expensive cost of surgery and long waiting lists along with fear of surgery especially for the elderly impede this treatment. An alternative treatment to reduce the urgency for replace surgery is needed.[24]

The medical treatment of cataract is one of the most important challenges in ophthalmic research.[25] Inhibitor E64 and its analogues have been developed and tested as the anti-cataract agents.[26] They are the epoxysuccinyl peptides and have electrophilic warheads that can interact with the active site of calpain irreversibly. However, because of their poor selectivity for calpains and cell impermeability, E64 has been established as unsuitable for development.

SJA6017 has been synthesized by Senju pharmaceutical and proved to be effective against selenite-induced cataract in rat.[27] Much work has been done in our research group to increase the potency, selectivity, and bioactivity of the lead inhibitor SJA6017. The first generation cataract inhibitors developed in the Abell/Coxon laboratory have an aldehyde warhead and a Val-Leu dipeptide core (**Figure 6**).

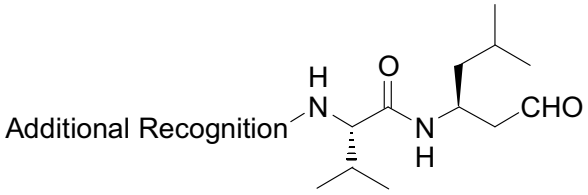

Figure 6: The first generation cataract inhibitors.

To increase the potency, cell permeability, water solubility, one strategy is to alter the left hand side (additional recognition). To date some 100 compounds of this type have been synthesized in our laboratory and assayed as inhibitors of calpain. These compounds are regarded as the first generation calpain inhibitors and have open chain structures. The compounds displaying nanomolar m-calpain inhibition constants (IC_{50}) that have comparable potency to SJA6017 are shown in **Figure 7**.

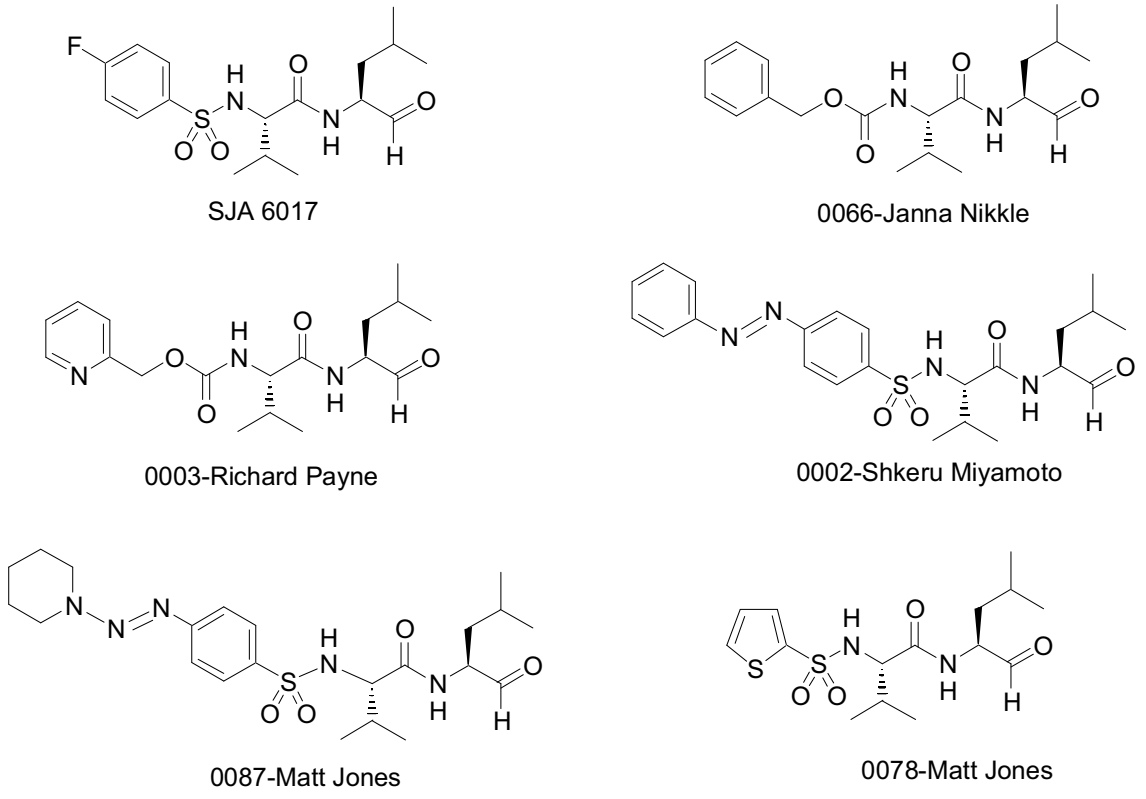

Figure 7: Nanomolar m-calpain inhibitors synthesised by the Abell/ Coxon research group.

To increase the biostability, β-amino acids can be introduced into peptide-based drugs since these compounds cannot be recognised by protease as being of peptide origin and thus remain stable in metabolism. A series of novel SJA6017 analogues were developed in our research group in an attempt to increase biostability.[28] This can be achieved by replacing the Val, Leu residues with the corresponding β-amino acids. However the inhibitor potency of these compounds was significantly lower.

1.5: The importance of a β-strand conformation for calpain inhibitors

The structure and conformation of an inhibitor plays an important role in its biological activity. This is because calpains can only recognize particular side chains and backbones and the interaction of inhibitor and calpain must present an entropy advantage. However most peptidic inhibitors are conformationally flexible and must present in a bioactive conformation before being recognized and bound by calpains. A kinetic study of protease-inhibitor complex formation (**Figure 8**) shows that inhibitor in a random conformation (I_{inact}) must convert to the active conformation (I_{act}) which is then bound by the enzyme to form the enzyme-inhibitor complex.

Calpain inhibitors should be designed such that the bioactive conformation is well populated thereby minimizing entropy loss on enzyme-inhibitor bonding.

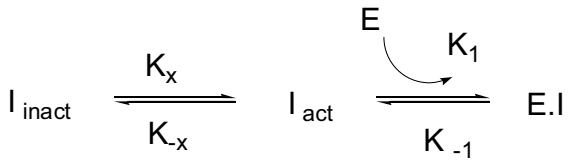

Figure 8: Conformational pre-equilibria of inhibitors and formation of protease inhibitor complex. I_{inact} / I_{act} is the inhibitor in inactive/active conformation.[29]

The β-strand conformation has potential in calpain inhibitor design. Fairlie *et al*. studied more than 1500 three dimensional X-ray structures of proteases in the Protein Data Bank and concluded that proteases universally bind the ligands in a β-strand conformation (**Figure 9a**).[30] This conformation prevents intramolecular hydrogen bonds of the adjacent amide bonds and optimizes the location of side chain residues for better bonding

to the proteases. The β-strand structure can be defined by bond angles Φ, ψ, and ω with optimum angles of -120°, 120° and 180° respectively (**Figure 9b**).

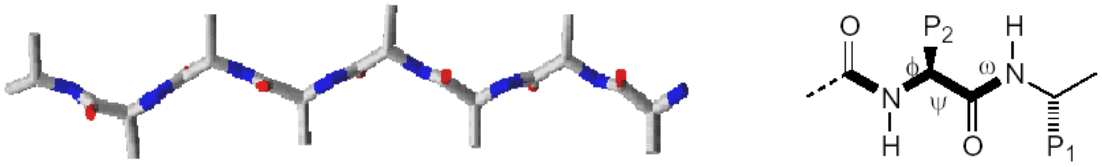

(a) (b)

Figure 9: (a) 3D structure of β-strand conformation; (b) β-strand backbone with torsional angles.

Population of a β-strand conformation is formed as the result of an extensive hydrogen bonding network and favorable side chain-side chain interactions. The residues in this conformation can be located at a right angle to the extended structure and thereby minimize steric interactions. The reason a ligand/inhibitor adopts such conformation is mainly due to the reduced loss of entropy for bonding.

For most of potent calpain inhibitors, three hydrogen bonds exist between inhibitor and Gly208 and Gly271 residues and the side chain functional groups must be in a specific arrangement to give rise to the β-strand geometry.

1.6: Literature Review of Calpain Inhibitors

Calpain inhibitors can be found in nature through screening, isolation, purification, and structure determination. Compound **1** was extracted from a streptomyces species and has been reported to inhibit calpain I and calpain II with Ki values of 36 nM and 50 nM respectively, however this compound is not selective for calpain and can also inhibit trypsin, chemotrypsin and cathepsin H.[31] Damnacanthal **2** was isolated from the root of Morinda citrifolia and is an effective calpain inhibitor; however, this compound has a poor selectivity since it inhibits other cysteine proteases.[32] Leupeptin **3** is the most widely known inhibitor and was isolated from streptomyces, however it displays no selectivity for calpain and the polarity of the arginine residue leads to the poor cell permeability (**Figure 10**).[33]

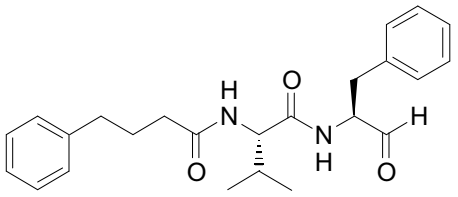

1

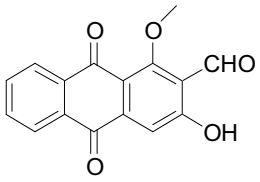

2

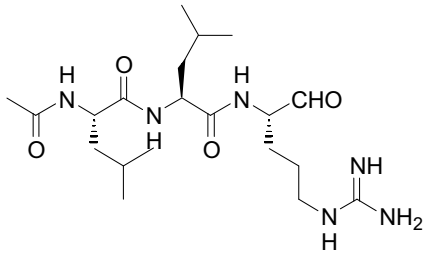

3

Figure 10: Typical calpain inhibitors from natural extraction.

Natural calpain inhibitors have limited potential for drug development because of their poor stability, solubility, selectivity and bioavailability. Therefore these inhibitor leads must be modified to have potential as therapeutic agents.

Synthetic calpain inhibitors can be divided into peptidic and non-peptidic compounds. The peptidic inhibitors consist of an address region for the enzyme recognition, namely a peptidic backbone that interacts with S_1 and S_2 subsites on calpain surface, and a warhead which can form a covalent bond either reversibly or irreversibly with the thiol group (-SH) of the active site of calpain.

The structures of two representative mercaptoacrylic acids **4**, **5** (shown in Figure 11) have the free thiol, carboxylate group and double bonds binding to the Ca^{2+} binding site.[34]

4 **5**

Figure 11: Non-peptidic calpain inhibitors.

Synthetic peptidic calpain inhibitors are classified into reversible (e.g. peptidyl aldehydes and peptidyl α-ketoamides) and irreversible inhibitors (e.g. peptidyl epoxides and β-fluoro ketones).[35]

Irreversible calpain inhibitors react with the Cys residue in the active site to form a permanent covalent bond. Examples of these include peptide epoxide inhibitors, azapeptides, and peptide acyloxymethyl. Because of the ubiquitous distribution of calpain isoforms, non-selective irreversible inhibitors have serious side effects.

Reversible inhibitors are preferable since they react with the enzyme's active site to form a stable but reversible species such as tetrahedral thiohemiacetal adduct. These adducts can resemble the transition states for substrate hydrolysis and thereby function as competitive inhibitors. Examples of reversible transition state inhibitors are peptide aldehydes,[36,37] α-diketones,[38] α-ketoesters, α-ketoamides and α-ketoacids.[39]

Classical peptidic calpain inhibitors are generally designed by replacing the scissile amide bond of calpain substrates with an electron deficient center (the warhead) (**Figure 12)**. The electron deficient center is usually an electrophilic carbonyl containing functional group (such as an aldehyde or a ketone) that can form a covalent bond either reversibly or irreversibly with the thiol group (-SH) of the active site Cys_{105} (m-calpain) or Cys_{115} (μ-calpain).

A peptidic calpain inhibitor has a peptidic backbone that interacts with S_1 and S_2 subsites on the calpain surface. Structure activity relationship (SAR) studies show that valine is preferable at the P_2 position, and the S_1 subsite of calpain can accommodate large hydrophobic groups from the P_1 position of inhibitors.[40] An aromatic group at *N*-terminal capping position seems to be favorable for binding to the S_3 subsites for the enzyme recognition (**Figure 12**).[8]

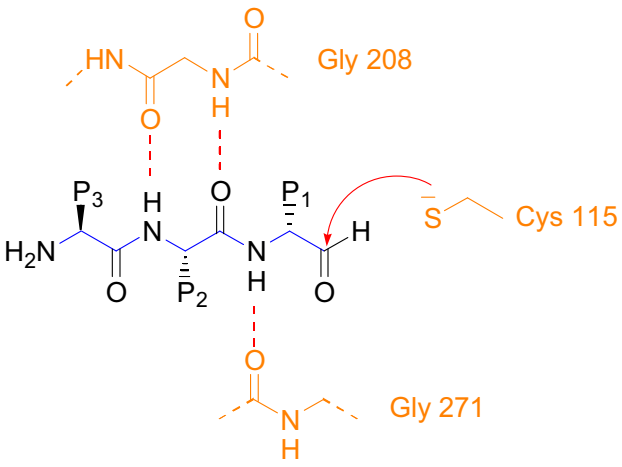

Figure 12: Design of peptidic calpain inhibitors.

A recent study of some 20 inhibitors including the measurement of IC_{50} values has been reported by Senju pharmacy Co Ltd. The IC_{50} values of these inhibitors containing an aldehyde warhead range from 7.5 to 630 nM, with the most potential being *N*-(4-fluorophenylsulfonyl)-L-valyl-L-leucinal (**6,** SJA6017) (**Figure 13**). Compound **6** was 10 times more potent against μ-calpain and twice as potent against m-calpain as any other calpain inhibitors tested. The synthetic calpain inhibitor **6** and its derivates can ameliorate cataractogenesis and diminish lens opacity in rats and porcine cataract models. However, this compound has poor membrane permeability, and bind to plasma proteins.

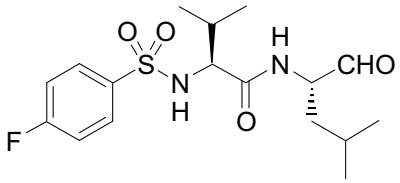

6

Figure 13: Structure of synthetic calpain inhibitor **6** (Senju Pharmaceuticals).

Compound **6** is a lead compound and structure activity relationship studies of analogous compounds were carried out by Senju Pharmaceuticals. A considerable amount of work to try to optimize a drug was reported but to date no compound has been tested in a clinical trial.

To improve the metabolic stability, Senju Pharmaceuticals prepared the cyclic hemiacetal **7**, nitrile **8**, and R-ketoamide **9** (**Figure 14**) and evaluated them as calpain inhibitors.[41] In this series, the aldehyde has been replaced because of its high activity which reacts superfluously with various substrates under physiological conditions. The hemiacetal **7** shows the most stability and has good water solubility, but is less potent than compound **6**.

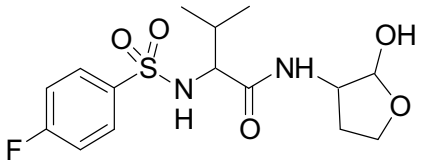

7

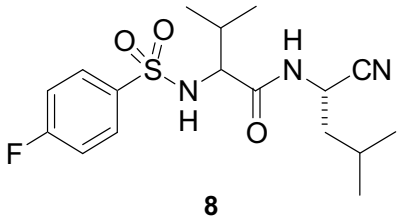

8

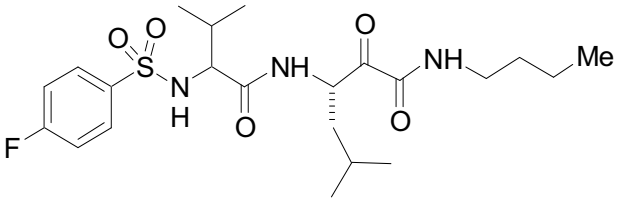

9

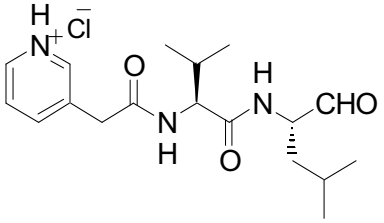

10

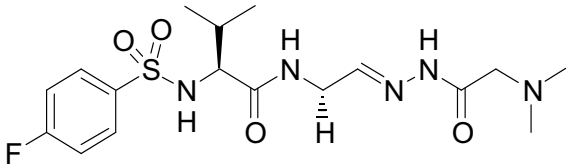

11

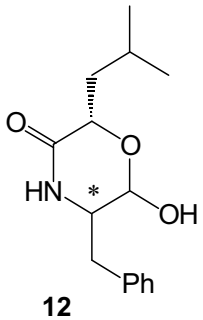

12

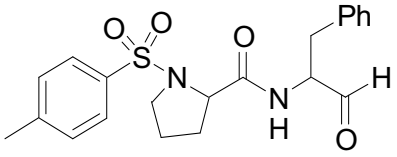

13

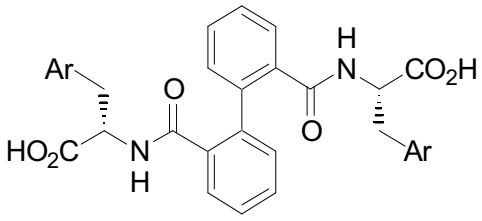

14

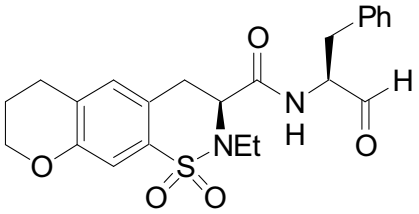

15

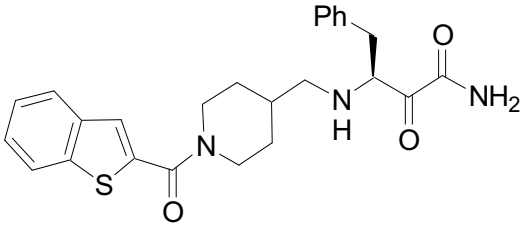

16

Figure 14: Calpain inhibitors.

Solubility is important since only compounds in solution are able to permeate across the cornea barrier.[42] To increase the water solubility alternative warheads were examined. Senju Pharmaceuticals examined peptidyl nitriles (**8**), α-ketoamides (**9**) and peptidyl hydrazones (**11**).[43] The hydrazone was a new template for calpain inhibition with N,N-dimethyl glycyl hydrazone **11** having appropriate water-solubility and being a potent inhibitor. Another way to increase the water-solubility was by incorporation of a pyridine ring at the P_3 site (**10**) but this compound exhibited only moderate activity.[44]

A series of 6-hydroxy-3-morpholinones has also been developed in which the aldehyde function group was converted to a cyclic hemiacetal (**Figure 15**).[45] Compared with the aldehyde inhibitors, the representative compound **12** (SNJ-1757) was more stable to nucleophilic attack and has a better corneal permeability.

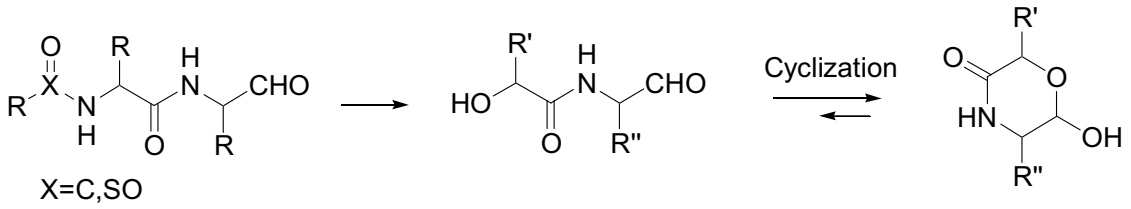

Figure 15: Synthesis of a prodrug cyclic hemiacetal.

Recently Tripathy et al. incorporated d-proline at the P_2 position of inhibitors to obtain potent calpain inhibitor **13**.[46] The calpain inhibitory potency should be dependent of the size of P_2 side chain. Compounds with a five-membered ring at the P_2 -position are more potent inhibitor and show 150-fold selectivity for calpain I over cathepsin B.

To improve the selectivity for μ-calpain, a series of urea-based peptidomimetic calpain inhibitors have been developed by replacement of P_2 chiral carbon with nitrogen (**Figure 16**). SAR shows that a benzyl group was preferred as the R_1 substituent, the iso-butyl

group was the preferred R_2 substituent and $PhCH_2O(CH_2)$ was introduced as R_3 substituent.[47]

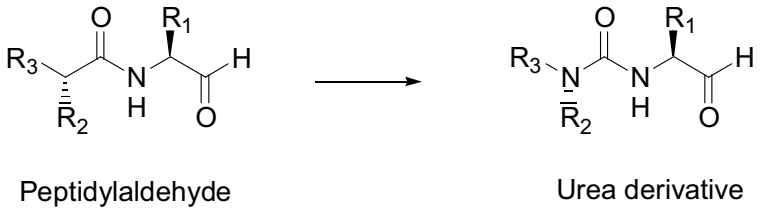

Figure 16

Peptide-biphenyl hybrids have been evaluated and shown to be potent and selective calpain inhibitors.[48] Unlike calpain inhibitors with electrophilic functionality, the aromatic groups in this species such as **14** interact with calcium binding sites rather than react directly with thiol group at the active site of calpain to hamper the activation of calpain. These compounds have been assayed and the IC_{50} values are in nanomolar scale. This strategy has increased the selectivity for calpain I over cathepsin B.

Ketoamide **15** was the most potent compound [IC_{50} (9 nM)] and functions as a reversible calpain inhibitor with a 300-fold selectivity for calpain over cathepsin B. The characteristic of this compound has been achieved by the substitution of the P_2 amino acid by peperidine carboxamides. P_2 and P_3 region can also be modified leading to a potent calpain inihibitor **16** which has a 150-fold selectivity for calpain I and vs. cathepsin B and reveals activity in cell culture.[49]

1.7: Molecular modeling and structure activity relationships

For our studies, the choice of a target compound for synthesis is a result of extensive molecular modelling to select molecules that well bind effectively in the active site of calpain. The X-ray structures of mini μ- and m-calpain mutant constructs (**Figure 17**) were used as a basis for molecular modeling. Examination of the structures reveals that the active site mini m-calpain calpain mutant construct is blocked by Trp_{106}. It is proposed that this obstruction was caused by instability of an α-helix adjacent to the active site. Therefore molecular modeling was performed using a mini μ-calpain construct which was prepared as follows: addition of hydrogens, conversion of the serine in the active site to a cysteine, relaxation or minimisation of the structure, and mapping the active site. Further improvements of this model were achieved through deprotonation of cystein, and protonation of histidine. Enzyme inhibition assays were performed by using m-calpain, isolated from sheep lung by Matthew Muir at Lincoln University.

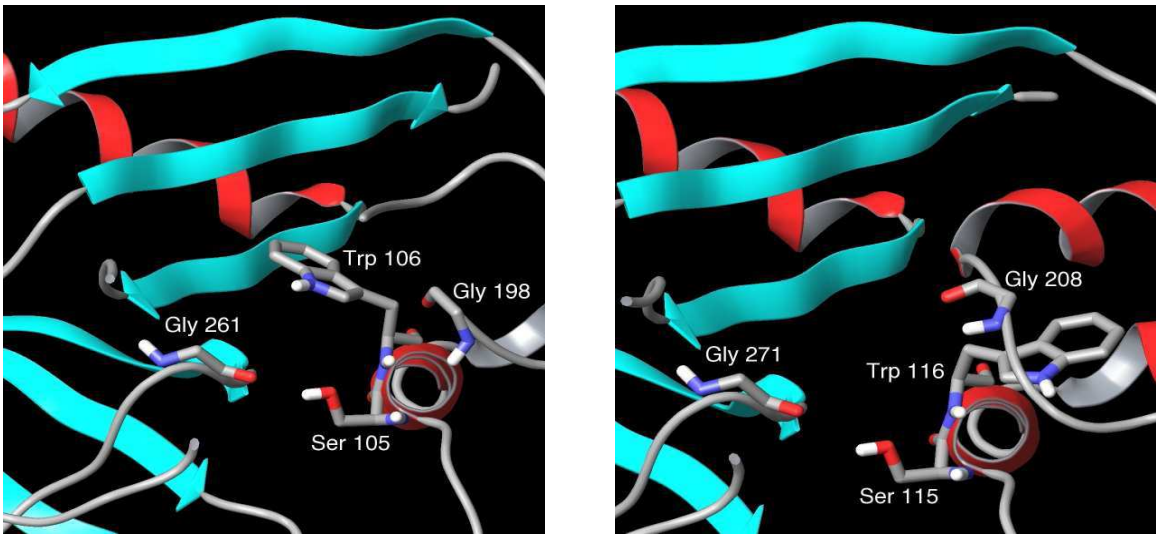

mini m-calpain **mini μ-calpain**

Figure 17: Mini-m and mini-μ calpain models.

Computational modeling entails the development in the computer of thousands of molecular poses for a given inhibitor. Ten or so lowest energy poses are selected for docking with the rigid model of calpain. There are several parameters obtained from the docking protocol. Glide scores reflect the binding energy especially the hydrogen bonds between ligands and the enzyme. It is not correlated with the IC_{50} value but good binders tend to have a Glide Score of less than -6; A potent inhibitor must have a warhead with appropriate position for nucelophilic attack by Cys_{115}, in other words, the distance of warhead to Cys_{115} should be less than 5Å. Visual and mathematical analysis of the molecule bound into the active site reveals whether or not it binds in a β-strand conformation. The docking results of the first generation calpain inhibitors (**Figure 7**) is given in **Table 2**, and shows some correlation with assay results.

Inhibitor	Glide score	H-bonding	Extra H-bonding	Warhead distance	IC_{50} (nM)
SJA6017	-6.6	A,B,C	0	3.94	80
0066-JN	-5.4	A,B,C	0	3.86	60
0003-RP	-6.2	A,B,C	1	3.78	80
0002-SM	-6.9	A,B,C	0	3.78	40
0078-MJ	-5.7	A,B,C	0	4.12	45
0087-MJ	-5.6	A,B,C	0	3.84	90

Table 2: Results of the first generation cataract inhibitors generated by Blair Stuart.

Rigid docking of some flexible ligands can give rise to anomalous results. The anticipated β-strand conformation, warhead distance, and glide score are not well correlated with the experimentally determined binding affinities. This can be explained by Koshland's theory of induced fit; that is, the substrate enters the active site and forces

it to take up the ideal shape to accommodate it. On the other hand, as the enzyme changes the shape to maximize the bonding interactions, it also alters the conformation of ligands. Induced fit docking can provide more accurate results but it is a much slower and more expensive docking protocol compared to the rigid docking.

1.8: References

[1] Azuma, M.; Fukiage, C.; David, L. L.; Shearer, T. R. *Exp. Eye Res*. **1997**, 64, 529-538.

[2] Donkor, I. O. *Current Medicinal Chemistry*. **2000**, 7, 1171-1188.

[3] Cuerrier, D.; Moldoveanu, T.; Davies, P. L. *The Journal of Biological Chemistry*. **2005**, 49, 40632–40641.

[4] Suzuki, K.; Hata, S.; Kawabata, Y.; Sorimachi, H. *Diabetes*. 2004, 53, (Suppl. 1): S12–S18.

[5] Moldoveanu, T.; Horsfiled, C. M.; Lim, D.; Elce, J. S.; Jia, Z.; Davies, P. L. *Cell*. **2002**, 108, 649–660.

[6] Schechter, I..; Berger, A. *Biochem. Biophys. Res. Comm*. **1967**, *27*, 157.

[7] Moldoveanu, T.; Hosfield, C. M.; Kim, D.; Elce, J. S.; Jia, Z.; Davies, P. L. *Cell*. **2002**, 649-660.

[8] Neffe, A. T.; Abell, A. D. *Current opinion in drug discovery & development*. **2005,** 8, 684.

[9] Wang, K. K.; Yuen, P.W. *Trends Pharmacol. Sci*. **1994**, 15, 412–419.

[10] Raynaud, F.; Marcilhac, A. *FEBS Journal*, **2006,** 273, 3437.

[11] Lee, M. S. et al. *Nature,* **2000**, 405, 360–364.

[12] Rami, A.; Agarwal, R., Botez, G.; Winckler J. *Brain Research*, **2000**, 866, 299–312.

[13] Biswas, S.; Harris, F.; Dennison, S.; Singh, J.; Phoenix, D. A. *Trends in molecular medicine.* **2004**, 10, 78-84.

[14] Huang, Y.; Wang, K.K. *Trends in Molecular Medicine*, **2001**, 355-362.

[15] Liu, F.; Grundke-Iqbal, I; Iqbal., K; Oda, Y.; Tomizawa, K.; Gong, C. X. *J. Bio .Chem.*, **2005**, 280, 37755-37762.

[16] Gafni, J.; Ellerby, L. M. *J. Neurosci*. **2002,** 22, 4842–4849.

[17] Mouatt-Prigent, A; Karlsson, J. O.; Agid, Y.; Hirsch E. C. *Neuroscience*, **1996**, 73, 979–987.

[18] González, A.; Sáez, M. E.; Aragón, M. J. J.; Galán, J.; Vettori, P.; Molina, L.; Rubio, C.; Real, L. M.; Ruiz, A.; Ramírez-Lorca, R. *Hum. Reprod.* **2006**, 21, 943–951.

[19] Biswas, S.; Harris, F.; Dennison, S.; Singh, J.; Phoenix, D. A. *Trends in Molecular Medicine*, **2004**, 10, 301-310.

[20] Benedek, G. B.; Pande, J.; Thurston, G. M.; Clark, J. I. *Progress in Retinal and Eye Research*, **1999**, 18, 391-402.

[21] Baruch, A.; Greenbaum, D.; Levy, E. T.; Nielsen, P. A.; Gilula, N. B.; Kumar, N. M.; Bogyo, M. *J. Biol. Chem*. **2001**, 276, 28999–29006.

[22] Morton, J. personal communication, **2005**.

[23] Mathur, O.; Suresh, K, G.; Wegener, A.R.; Breipohl, W.; Ahrend, M.H.; Sharma, Y.D.; Gupta, Y. K.; Vajpayee, R. B. *Curr. Eye Res*. **2000**, 21, 926.

[24] Olson, R. J.; Mamalis, N.; Werner, L.; Apple, D. *J. Am. J. Opth*. **2003**, *136*, 146.

[25] www.nzine.co.nz/features/cataractresearch.html.

[26] Azuma, M.; David, L. L.; Shearer, T. R. *Biochim. Biophys. Acta* **1992**, 1180, 215–220.

[27] Tamada, Y.; Fukiage, C.; Mizutani, K.; Yamaguchi, M.; Nakamura, Y.; Azuma, M.; Shearer, T. R. *Current Eye Research.* **2001**, 22, 280-285.

[28] Payne, R. J.; Brown, K. M.; Coxon, J. M.; Morton, J. D.; Lee, H. Y.; Abell, A. D. *Aust. J.Chem.*, **2004**, 57, 877-884.

[29] Fairlie, D. P.; Tyndall, J. D. A.; Reid, R. C.; Wong, A. K.; Abbenante, G.; Scanlon, M. J.;

March, D. R.; Bergman, D. A.; Chai, C. L. L.; Burkett, B. A. *J. Med. Chem.* **2000**, *43*, 1271-1281.

[30] Tyndall, J.; Fairlie, D. P. *J. Mol. Recognit*, **1999**, 12, 363-370.

[31] Sasaki, T.; Kishi, M.; Saito, M.; Tanaka, T.; Higuchi, N.; Kominami, E.; Katunuma, N.; Murachi, T. *Journal of Enzyme Inhibition*. **1990**, 3, 195-201.

[32] Hiwasa, T.; Takeda, A.; Umezawa, K. *Journal of Biochemistry, Molecular Biology and Biophysics*, **1999**, 2, 311-316.

[33] Fukiage, C.; Azuma, M.; Nakamura, Y.; Tamada, Y.; Nakamura, M.; Shearer, T. R. *Biochimica et Biophysica Acta*, **1997**, 1361*,* 304–312.

[34] Schirmeister, T.; Kaeppler, U.; *Mini Reviews in Medicinal Chemistry,* **2003**, 3, 361-373.

[35] Biswas, S.; Harris, F.; Dennison, S.; Singh, J.; Phoenix, D. A. *Trends in molecular medicine.* **2004**, 10, 78-84.

[36] Woo, J. T.; Sigeizumi, S.; Yamaguchi, K.; Sugimoto, K.; Kobori, T.; Tsuji, T.; Kondo, K. *Bioorg. Med. Chem. Lett*. **1995**, 5, 1501-1504.

[37] Iqbal, M.; Messina, P. A.; Freed, B.; Das, M.; Chatterjee, S.; Tripathy, R.; Tao, M.; Josef, K. A.; Dembofsky, B.; Dunn, D.; Griffith, E.; Siman, R.; Senadhi, S. E.; Biazzo, W.; Bozyczko-Coyne, D.; Meyer, S. L.; Ator, M. A.; Bihovsky, R. *Bioorg. Med. Chem. Lett.* **1997**, 7, 539-544.

[38] Chatterjee, S.; Iqbal, M.; Mallya, S.; Senadhi, S. E.; O'Kane, T. M.; McKenna, B.A.; Bozyczko-Coyne, D.; Kauer, J. C.; Siman, R.; Mallamo, J. P. *Bioorg. Med. Chem.* **1998**, 6, 509-22.

[39] Li, Z.; Patil, G. S.; Golubski, Z. E.; Hori, H.; Tehrani, K.; Foreman, J. E.; Eveleth, D. D.; Bartus, R. T.; Powers, J. C. *J. Med. Chem.* **1993**, 36, 3472-3480.

[40] Inoue, J.; Nakamura, M.; Cui, Y-S.; Sakai, Y.; Sakai, O.; Hill, J. R.; Wang, K. W. W.; Yuen, P-W. *J. Med. Chem.* **2003**, 46, 868-871.

[41] Shirasaki, Y.; Nakamura, M.; Yamaguchi, M.; Miyashita, H.; Sakai, O.; Inoue, J. *J. Med. Chem*., **2006**, 49, 3926-3932.

[42] Di, L.; Kerns, E. H. *Drug Discovery Today*. **2006**, 11, 446-451.

[43] Shirasaki, Y.; Nakamura, M.; Yamaguchi, M.; Miyashita, H.; Sakai, O.; Inoue. J. *J. Med. Chem.* **2006**, 49, 3926-3932.

[44] Nakamura, M.; Yamaguchi, M.; Sakai, O.; Inoue, J. *Bioorg. Med. Chem.* **2003,** 11, 1371–1379.

[45] Nakamura, M.; Miyashita, H.; Yamaguchi, M.; Shirasaki, Y.; Nakamura, Y.; Inoue, J. *Bioorganic & Medicinal Chemistry.* **2003,** 11, 5449–5460.

[46] Donkor, I. O.; Korukond, R.; Huang, T. L. *Bioorg. Med. Chem. Lett*. **2003**, *13*, 783–784.

[47] Sanders, M. L.; Donkor, I. O. *Bioorg. Med. Chem. Lett*. **2006**, *16*, 1965–1968.

[48] Montero, A.; Alonso, M.; Benito, E.; Chana, A.; Mann, E.; Navasb, J. M.; Herradona, B. *Bioorg. Med. Chem. Lett.,* **2004**, *14*, 2753–2757.

[49] Hernandez, A. A.; Roush, W. R. *Current Opinion in Chemical Biology,* **2002**, 6, 459–465.

Chapter 2: Results and discussion

2.1: Synthesis

The Val-Leu dipeptidyl aldehydes **33a-e, 33g, 33i** and **35** have been synthesized. These target molecules were chosen as a result of molecular modeling studies (see section: **2.3**). They share common characteristics in that modeling studies suggests that the bioactive β-strand conformation is dominant in the conformational ensemble, that they will have suitable binding affinity to the enzyme and an appropriate warhead distance from the active site cysteine sulphur of the active site of calpain.

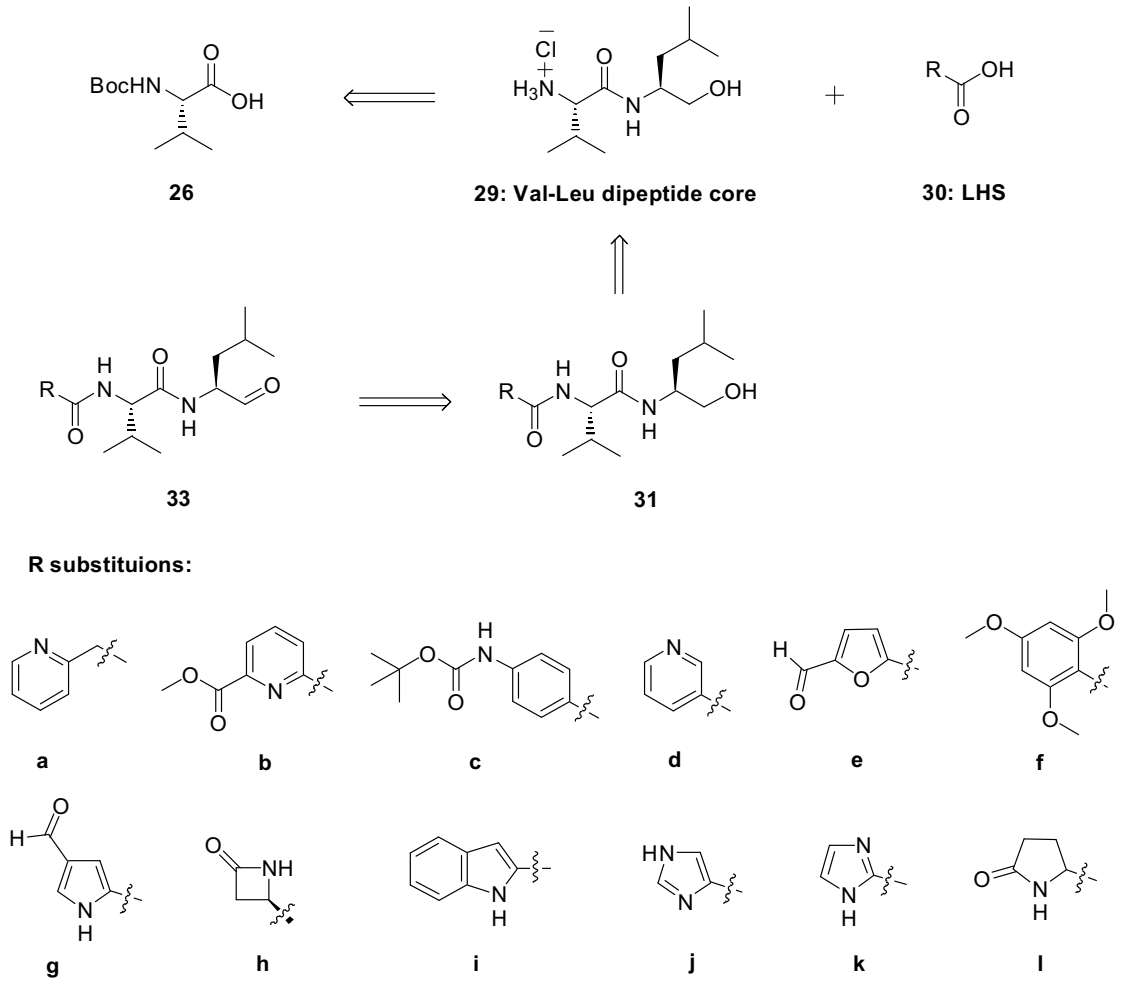

Figure 18: Retrosynthetic analysis of the Val-Leu dipeptidyl aldehydes (**Series 33**).

The discussion covers first the preparation of the carboxylic acids **17, 18,** and **19** that were not commercially available and which form the left hand side (LHS) address region for some of the compounds we planned to study (see **2.1.1**). This is followed by the preparation of the Val-Leu dipeptide core **29**, and the Val-Leu dipeptidyl alcohols (**31a-g** and **31i**). Finally we discuss the last step in the synthesis of the Val-Leu dipeptidyl aldehydes **33a-e, 33g, 33i** and **35** (**Figure 18**).

2.1.1: Synthesis of LHS starting materials

Specifically the series of Val-Leu dipeptidyl aldehydes **33a-l,** have been made to investigate the effect of left hand side address region on the inhibition of the cysteine protease, m-calpain. The left hand side groups are all derived from carboxylic acids that are deemed capable of forming appropriate hydrogen bonding interactions with the S_3 pocket of m-calpain. In addition to nicotinic acid, pyridylacetic acid, and furan carboxylic acid which are commercially available, carboxylic acids **17, 18,** and **19** containing pyridine, benzene and pyrrole groups were prepared.

Modelling studies show that an aromatic group at left hand side is likely to bind to the S_3 subsites of the enzyme. It is expected that the carbonyl groups of the pyridine carboxylic acid **17** and 2-pyrrole carboxylic acid **19** will contribute to H-bonding and facilitate an extended β-strand conformation of the inhibitor upon binding to m-calpain. The pyrrole **19** and amine **18** similarly have the capacity of forming the H-bonds in the S_3 pocket (**Figure 19**).

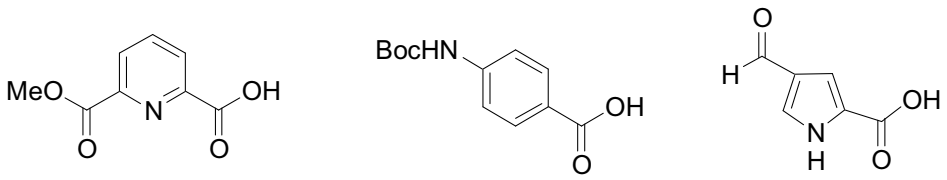

17 **18** **19**

Figure 19: Structure of synthesized left hand side starting materials.

The carboxylic acid **17** was prepared (**Scheme 2)** from commercially available pyridine-2, 6-dicarboxylic acid **20** which was converted to the dimethyl ester **21** with methanol in the presence of thionyl chloride. A 6-H singlet in the ^{1}H NMR spectrum at 3.9 ppm indicates the formation of the diester. Selective monohydrolysis using the method developed by Schmuck[50] gave 2,6-pyridinedicarboxylic acid, mono methyl ester **17** as the sole product (98%) again confirmed by integration of the methyl ester peak in the ^{1}H NMR.

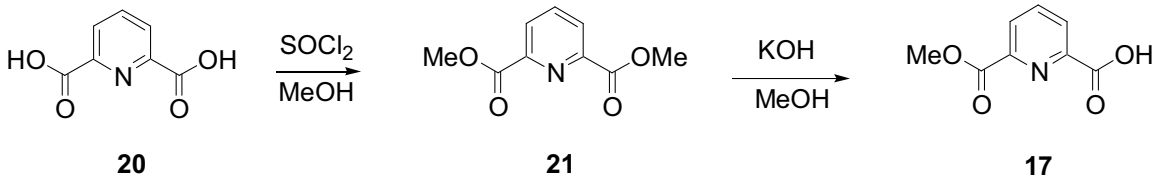

20 **21** **17**

Scheme 2: Synthesis of LHS **17**.

In an attempt to synthesize 4-(*N*-tert-Butoxycarbonyl) aminobenzoic acid **18**, BOC protection of 4-amino-benzoic acid methyl ester **22** was attempted (**Scheme 3).** The aminoester **22** in dioxane was stirred at room temperature for 18 hrs with sodium hydroxide (4 equiv) predissolved in distilled water and di-tert-butyl dicarbonate (4 equiv) added. This procedure failed and resulted only in the isolation of starting material. An alternative protection method was attempted where ester **22** was reacted with tert-butoxycarbonyl in the presence of DMAP as catalyst. This reaction yielded a mixture of mono **23** and di **23a** protected products. Purification of these compounds was not attempted as literature precedence[51] indicated a second BOC group on an amine is base labile and the next step in the synthesis of **18** was a base mediated ester hydrolysis. A mixture of **23** and **23a** was therefore hydrolyzed with an excess of base (4 equivalents) to give corresponding mono BOC protected aminobenzoic acid **18** in excellent yield (89%).

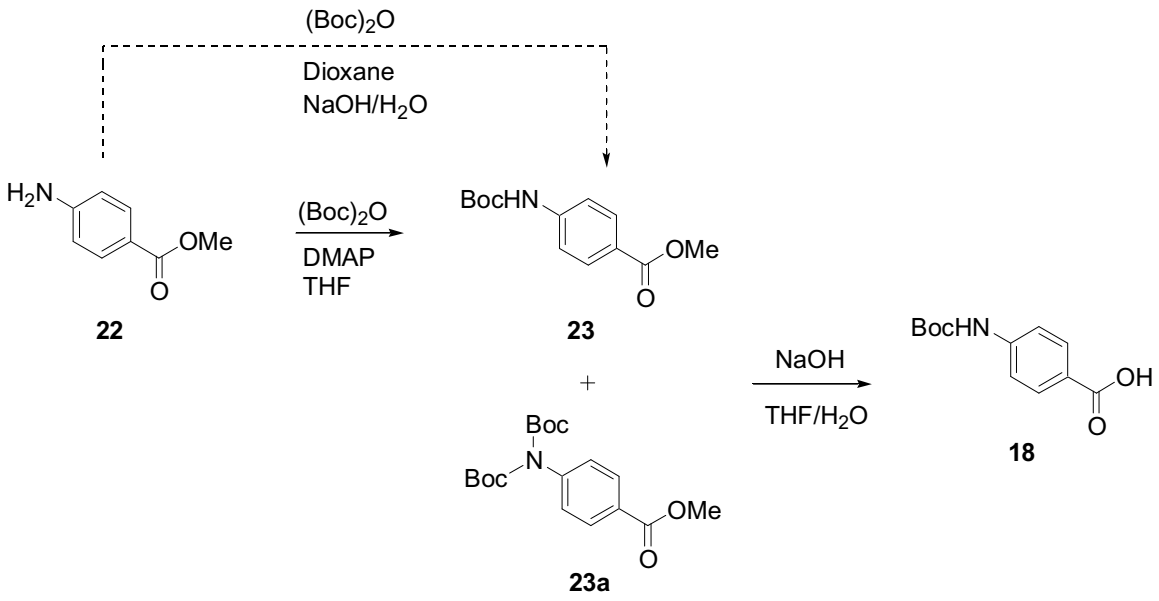

Scheme 3: Synthesis of the LHS **18**.

BOC protection of aminobenzoic methyl ester **22** is catalyzed by DMAP via acylation of the pyridine ring to give a highly reactive pyridinium species which undergoes nucleophilic attack by amine to give **23** at the same time regenerating the catalyst (**Scheme 4**).[52] The presence of the BOC group was confirmed by the appearance of a large singlet at 1.45 ppm in ^{1}H NMR spectra.

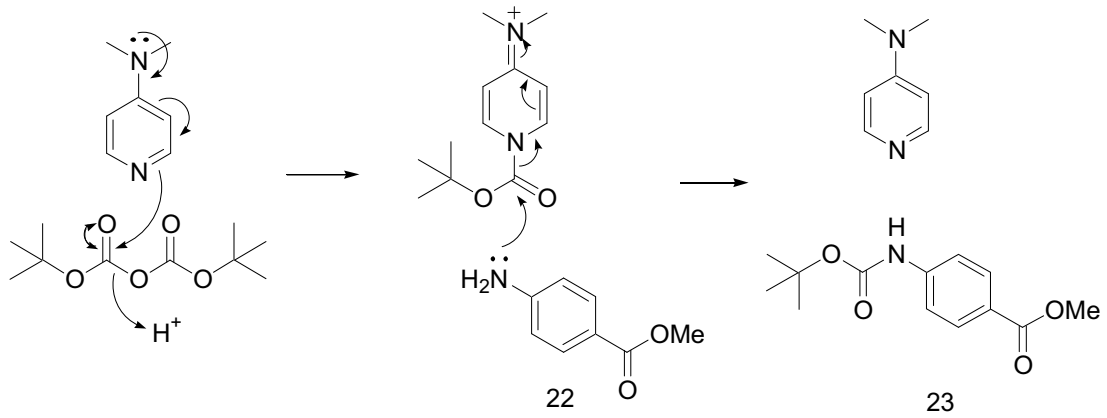

Scheme 4: BOC protection catalyzed by DMAP.

The synthesis of 4 –formyl-pyrrole-2-carboxylic acid **19** was achieved *via* hydrolysis of the corresponding ester **25** in an excellent yield (85%) (**Scheme 5**). The starting ester **25** was synthesized using a formylation reaction of 2-pyrrole ethyl ester **24** followed by chromatographic separation of the 4- and 5-formyl isomeric mixture.

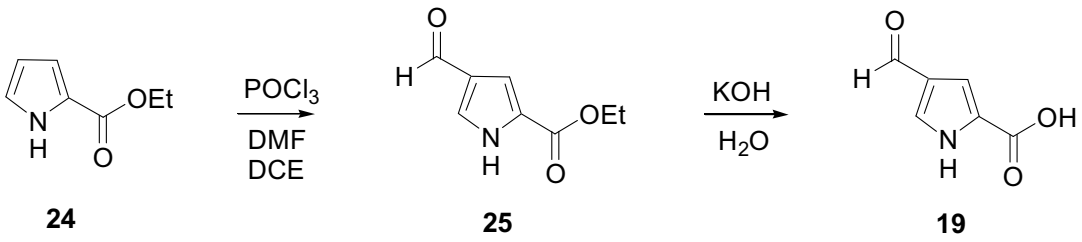

24 **25** **19**

Scheme 5: Synthesis of LHS **19.**

2.1.2: Synthesis of Val-Leu dipeptide core

Inhibitors can be schematically divided into LHS, dipeptide core and warhead (**Figure 20**). Various aromatic groups have been designed and substituted at the left hand side of inhibitors for enzyme recognization. Aldehyde has been used as a warhead since this electrophilic carbonyl group can form reversible covalent adduct with the active cysteine site of calpain. The peptide core consists of a Val-Leu dipetide and is believed to exhibit favourable hydrophobic interaction in the S_1 and S_2 pockets of m-calpain.

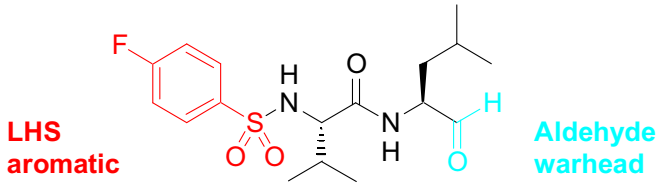

Figure 20: Val-Leu dipeptidyl aldehyde.

The Val-Leu dipeptide core **29** was synthesized by coupling of commercially available Boc-Valine **26** and L-Leucinol **27** to give N-Boc-Val-Leu-OH **28** (54%) which after hydrolysis gives the hydrochloride salt **29** (**Scheme 6**).

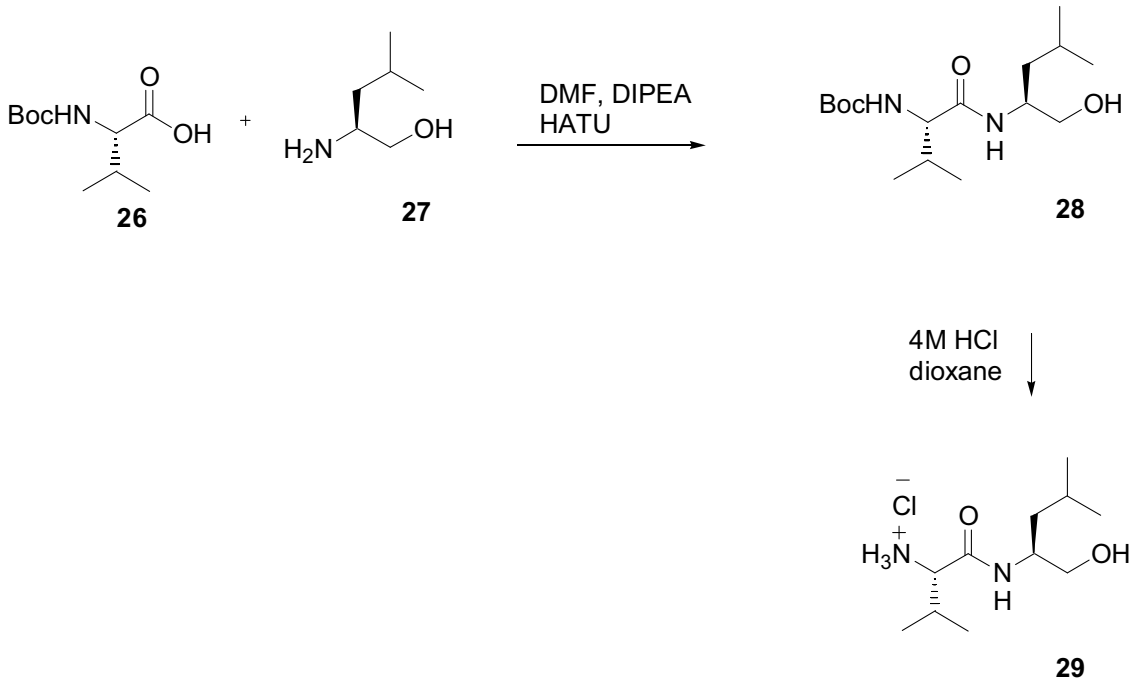

26 **27** **28** **29**

Scheme 6: Synthesis of the dipeptide core hydrochloride salt **29.**

The peptide coupling reaction to give dipeptides **28** was carried out under mild conditions using HATU as the coupling regent. This reaction proved to be robust and multigram quantities (>10g) of **28** were prepared.

Acidolysis of BOC-dipeptide **28** by hydrogen chloride is employed to remove tert-buoxycarbonyl group. The cleavage is initiated by protonation of the carbonyl followed by electron shift to give a carbenium ion. The carbenium ion is fragmented into *tert*-butyl cation followed by reaction with a nucleophile chloride counter-ion to give *tert*-butyl chloride (S_N2 mechanism) and acid carbonate. The acid carbonate has a hemiacetal structure which is easy to decompose to liberate carbon dioxide (**Scheme 7**).[53] Deprotection of **28** to give amine salt **29** is usually carried out at 60^{o}C since the

carbenium ion is relatively stable and usually requires heat for fragmentation. The removal of the BOC group can be seen by the disappearance of a large singlet at 1.3 ppm in ^{1}H NMR spectrum.

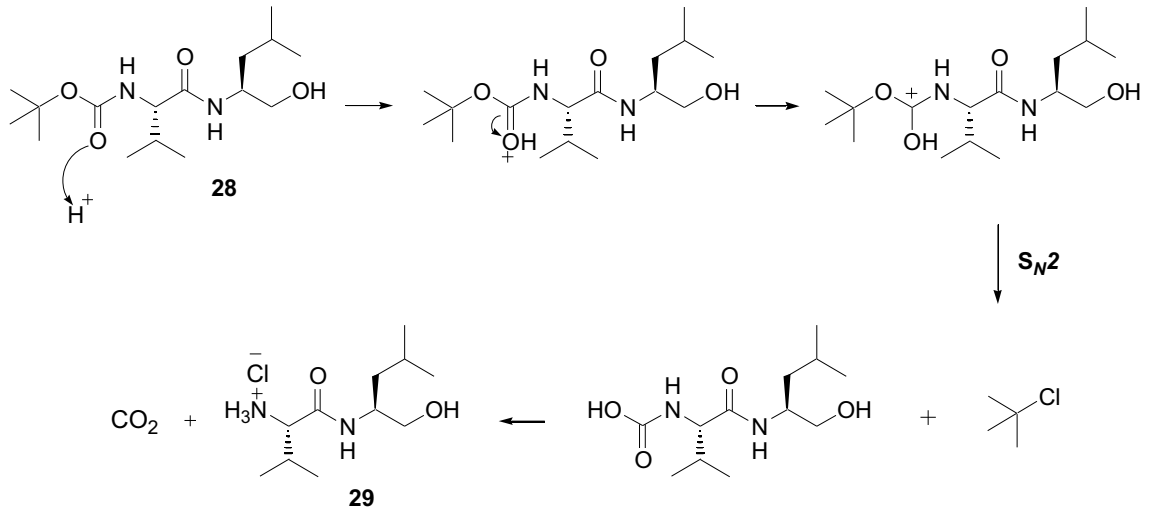

Scheme 7: Deprotection of BOC by acidolysis.

2.1.3: Synthesis of Dipeptidyl Alcohols

The Val-Leu dipeptide alcohols **31a, 31b, 31c, 31d, 31e, 31f, 31g** and **31i** were prepared by coupling the hydrochloride salt **29** with corresponding carboxylic acids **30** using HATU or EDC as coupling reagents (**Scheme 8**).

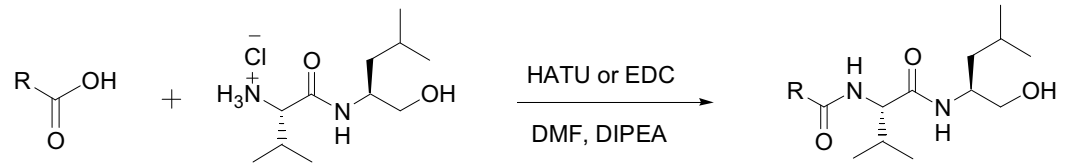

30: LHS **29:** Dipeptide core **31**: Dipeptidyl alcohols

30a: 2-pyridylacetic acid — **31a**
17: pyridine-2,6-dicarboxylic acid monomethyl ester — **31b**
18: 4-tert-butoxycarbonylamino-benzoic acid — **31c**
30d: nicotinic acid — **31d**
30e: 5-formyl-furan-2- carboxylic acid — **31e**
30f: 2,4,6-trimethoxy-benzoic acid — **31f**
19: 4-formyl-1H- pyrrole- 2- carboxylic acid — **31g**
30i: indole-2-carboxylic acid — **31i**

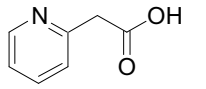

30a: 2-pyridylacetic acid

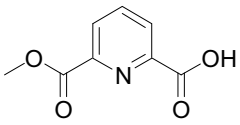

17: pyridine-2,6-dicarboxylic acid monomethyl ester

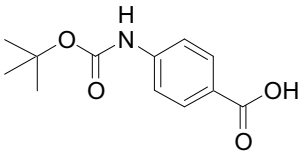

18: 4-tert-butoxycarbonyl amino-benzoic acid

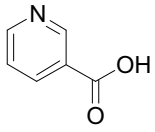

30d: nicotinic acid

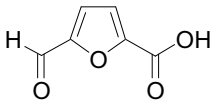

30e: 5-formyl-furan-2-carboxylic acid

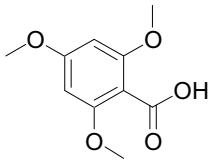

30f: 2,4,6-trimethoxy-benzoic acid

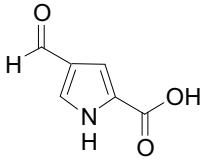

19: 4-formyl-1H-pyrrole - 2- carboxylic acid

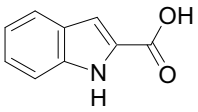

30i: indole-2-carboxylic acid

Scheme 8: Synthesis of amino alcohols **31a-31l.**

An important strategy for the synthesis of these dipeptidyl alcohols **31a-l** is the choice of coupling regent as this can affect yield and stereochemistry. HATU is an efficient coupling regent for coupling sterically hindered amino acids.[54] The mechanism of HATU coupling is shown in **Figure 21**.

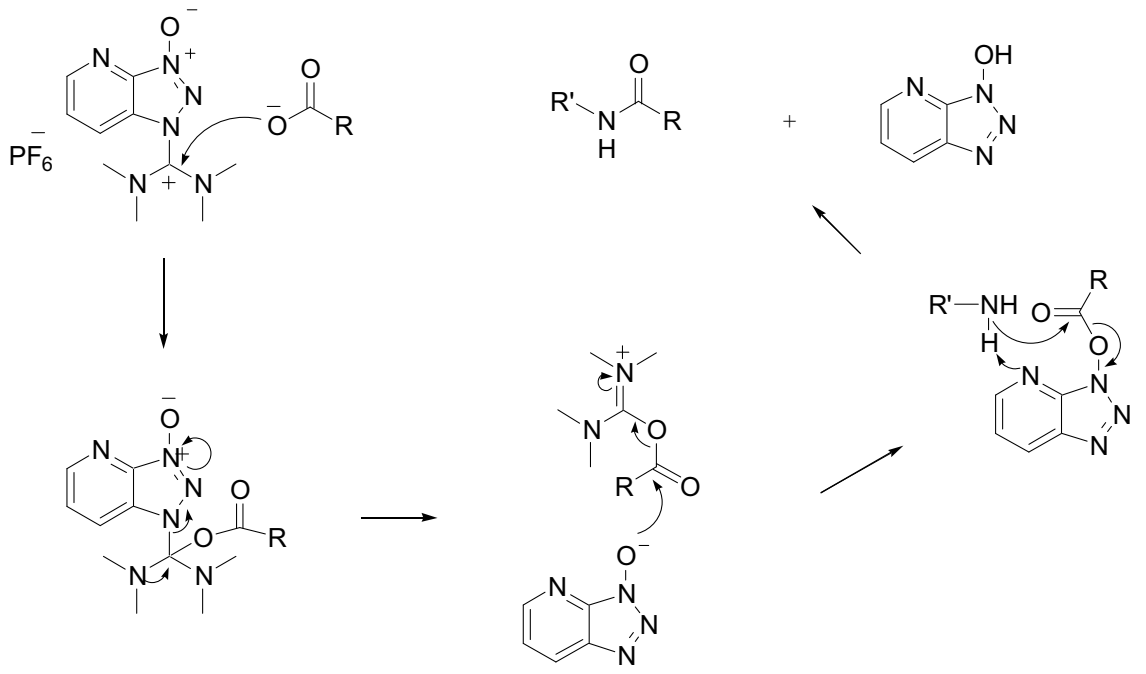

Figure 21: General mechanism of HATU coupling reactions.

HATU was employed as the peptide coupling regent for the synthesis of Val-Leu dipeptidyl alcohols **31b** and **31c.** Compound **31b** was prepared by coupling pyridine carboxylic acid and dipeptide core **29** (83% yield). 4-tert-Butoxycarbonylaminobenzoic acid was coupled with **29 to** give **31c** (65%) (**Scheme 9**).

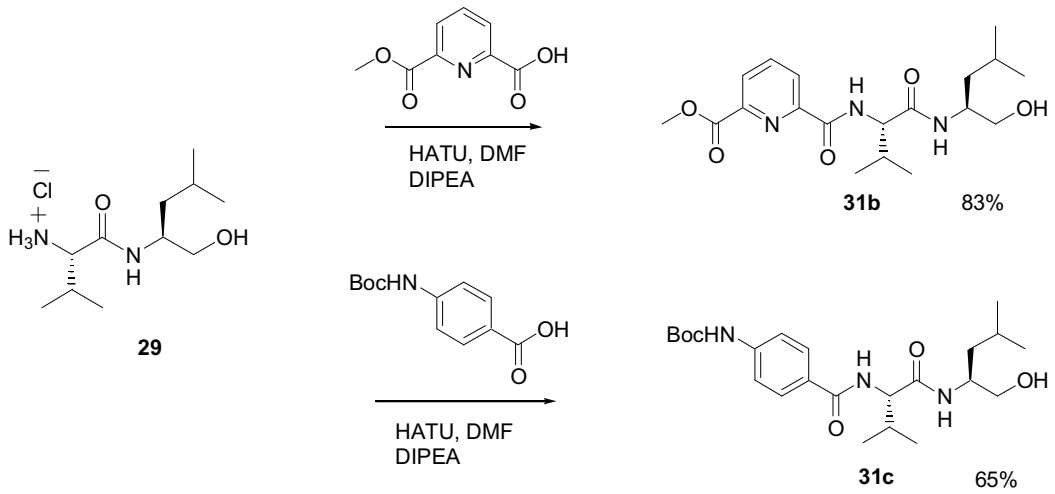

Scheme 9: Synthesis of amino alcohols **31 b** and **31c.**

HATU is a highly reactive coupling reagent and in some cases can give rise to undesired side reaction (**Scheme 10).** Commercially available nicotinic acid reacted with **29** in the presence of HATU as a coupling regent and gave the desired amino alcohol **31d**, however the ^{13}C NMR of the product showed that esterification had occurred to form a mixture of compounds **31d** and **32**. The spectrum shows four carbon signals corresponding to the two α-carbons of the two products (60.18, 60.22, 64.27 and 66.64 ppm) (**Figure 22**).

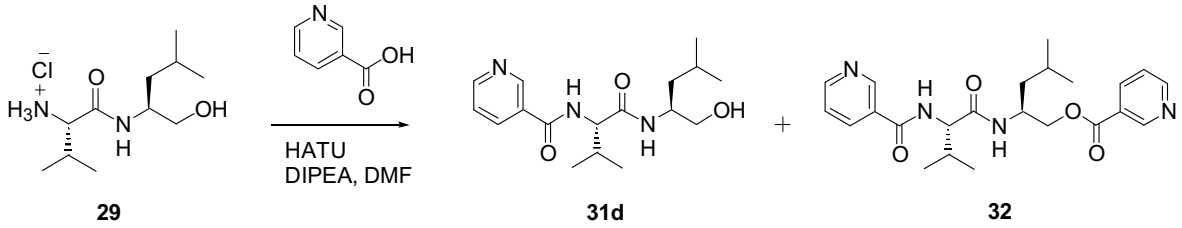

29 **31d** **32**

Scheme 10: HATU coupling of nicotinic acid to dipeptide **29**.

Figure 22: Section of the ^{13}C NMR spectrum of the HATU mediated coupling of nicotinic acid to dipeptide **29**.

Due to the esterification side reaction using HATU chemistry, a coupling reaction of nicotinic acid with dipeptide **29** was performed using EDC/HOAt and with EDC/HOBt in an attempt to make **31d** in the absence of ester (**Scheme 11**).

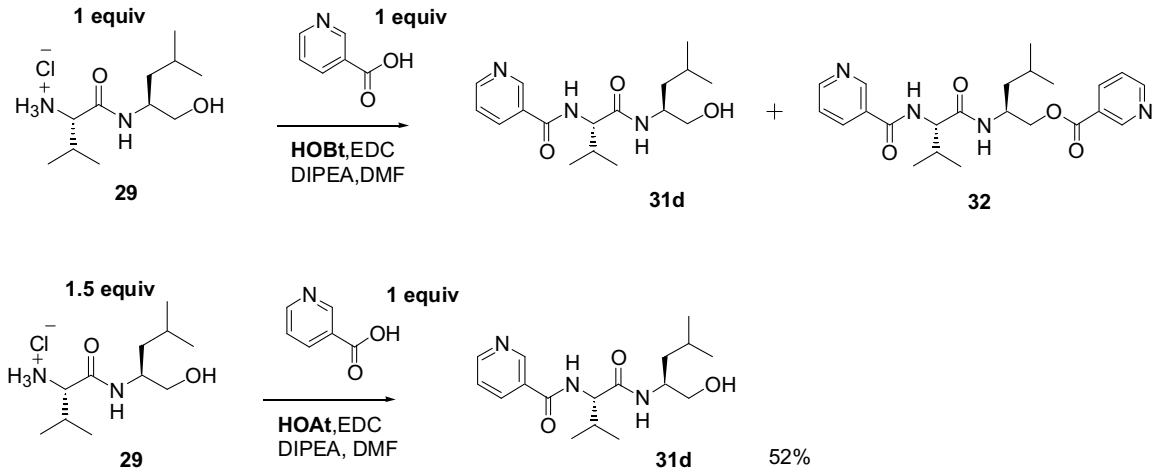

Scheme 11: Synthesis of amino alcohol **31d** using a variety of coupling conditions

An EDC/HOBt coupling of nicotinic acid to dipeptide **29** again resulted in some esterication. However, an EDC/HOAt mediate coupling reaction where the stoichoimetry of the reagents had been changed from 1:1 equivalents (dipeptide:nicotinic acid) to 1.5:1 resulted only in the formation of **31d**. The ^{13}C NMR spectrum of the EDC/HOAt reaction clearly shows that no esterification had occurred and only **31d** was formed. Only two α-carbon signals can be observed (60.16 and 64.25 ppm) (**Figure 23**).

Figure 23: Section of the ^{13}C NMR spectrum of the EDC/HOAt mediated coupling of nicotinic acid to dipeptide **29**.

Based on the above results, EDC/HOAT mediated coupling was used for the synthesis of **31e-i.** Compound **31e** was synthesized by coupling 5-formyl-furan-2-carboxylic acid and dipeptide core **29** (31%). Compound **31f** was obtained by condensation of 2,4,6-trimethoxy-benzoic acid and compound **29** (76% yield). 4-Formyl-1H-pyrrole-2-carboxylic acid and 1H-indole-2-carboxylic acid were coupled with core **29** to give compounds **31g** and **31i** (36% and 70% respectively) (**Table 3**). A pure sample of compound **31h** was not obtained as the product from peptide coupling was water soluble resulting in difficult extraction, separation and purification from the by-products of reaction. Examination of the ^{13}H NMR of compounds **31e-g** and **31i** showed no evidence of esterification.

Compound **31a** was prepared in 43% yield by reaction of 2-pyridylacetic acid and dipeptide core **29** effected by EDC/HOAT. The yield was improved to 61% by using the phosphonium reagent PyBroP as coupling reagent.

The yields of the Val-Leu dipeptidyl alcohols **31a-l** are summarized in **Table 3**.

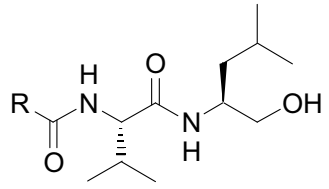

31: dipeptidyl alcohols

No.	R	Structure	Yield
31a	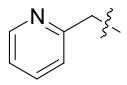	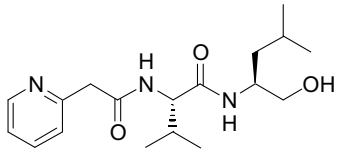	61%
31b	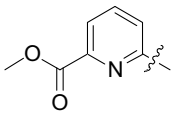	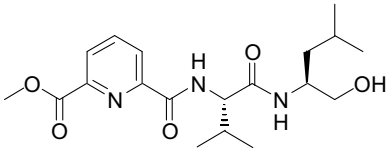	83%
31c	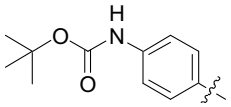	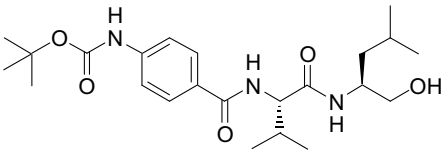	65%
31d		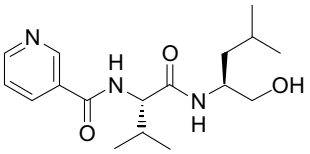	52%
31e	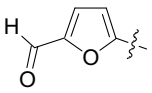	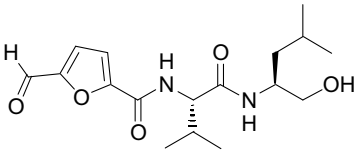	31%
31f	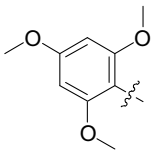	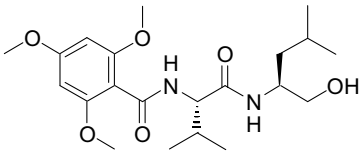	76%
31g	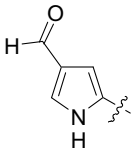	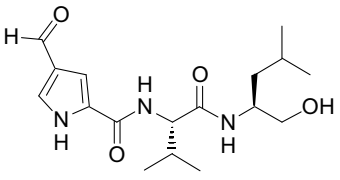	36%
31h		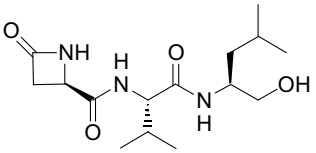	Not isolated

31i	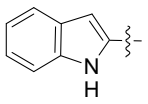	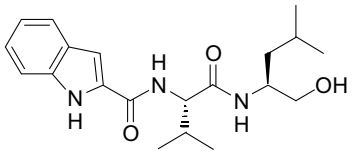	70%
31j	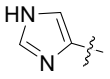	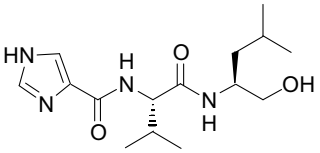	0%
31k	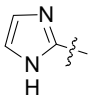	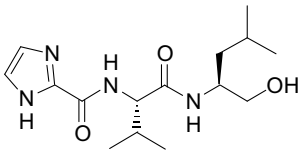	0%
31l	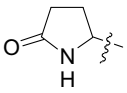	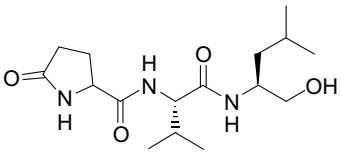	Trace amounts

Table 3: Yields for the synthesis of amino alcohols **31a-l.**

Conventional coupling procedures are not suitable in the synthesis of compounds **31j** and **31k** since imidazole-carboxylic acid has poor solubility in DMF. A potential alternative synthesis of **31j** and **31k** is to utilize microwave irradiation with HOBT and di-isopropylcarbodiimide (DIC) as coupling reagents. Microwave irradiation has been employed in several cases to direct condensation of amines and carboxylic acids.[55] Peptide coupling reactions under microwave irradiation can reduce the reaction time, reduce side reactions, and increase the yield of product and sometimes proceed even without an activation catalyst.[56] However, due to time constraints microwave chemistry was not attempted.

The synthesis of compound **31l** was attempted using HATU and EDC/HOAT regents under a mild condition, however, no coupled product was observed. Coupling reactions involving pyroglutamic acid are notoriously difficult. A alternative method synthesize compound **31l** was made using the method developed by David *et al* [57] at 0 °C using HATU but only trace amounts of the product were formed. ^{1}H NMR and TLC analysis shows that the isolated material was mainly unreactived starting material. An alternative method for coupling on a small scale in DMF using HBTU is known; however, as large quantities of **31l** are required this method was not attempted.[58]

2.1.4: Synthesis of Val-Leu dipeptidyl aldehydes

The dipeptidyl alcohols **31a-l** were oxidized with activated dimethyl sulfoxide (DMSO) to the corresponding dipeptidyl aldehydes **33a-g,** and **33i.** These aldehydes were assayed against m-calpain to measure their ability to act as inhibitors (**Scheme 12**).

Scheme 12: General procedure for the oxidation of amino alcohols **31a-l**

Dimethyl sulfoxide (DMSO) as an oxidizing reagent can be activated by several electrophlies such as dicyclohexylcarbodiimide (DCC),[59] acetic anhydrid,[60] phosphorous pentoxide,[61]trifluoroacetic anhydride,[62]oxalyl chloride,[63] and complex SO_3.Pyr.[64] The activated DMSO can react with a primary alcohol to form the corresponding aldehyde or ketone.

Swern oxidation with oxalyl chloride as activator was attempted for the oxidation of **31a**, but the yield was low. This is probably due to the sensitivity of the method to moisture and temperature. The reaction is carried out at minus 60°C because that oxalyl chloride is a strong activator and the resulting highly reactive DMSO complex can decompose to the methylene sulfonium salt. Pummerer rearrangement occurs if temperature is above -60°C (**Figure 24**).

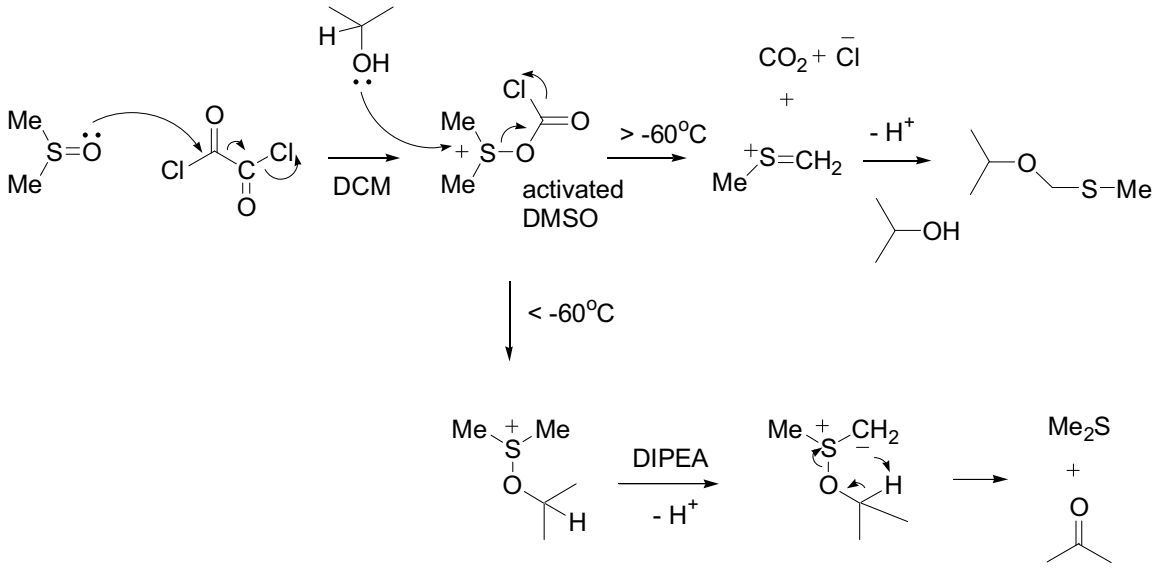

Figure 24: Swern oxidation pathway and Pummerer rearrangement.

Compared with oxalyl chloride, SO_3/pyridine is a mild activator and can activate DMSO even at room temperature. The resulting activated DMSO is less reactive and methylene sulfonium salt is less easily formed. Oxidation of **31a** with SO_3/pyridine complex was carried out to give **33a** in 45% yield indicating it to be more effective than Swern oxidation (**Scheme 13).** Therefore this method is used for amino alcohols **31a-f**, **31g** and **31i.** The best yield was obtained using a mixture of DMSO/DCM (2:1) as solvent. The reaction should be cooled on ice bath for 2 hours. However, all attempts to oxidize **31f** under these conditions failed. No explanation for this apparent lack of activity can be proposed.

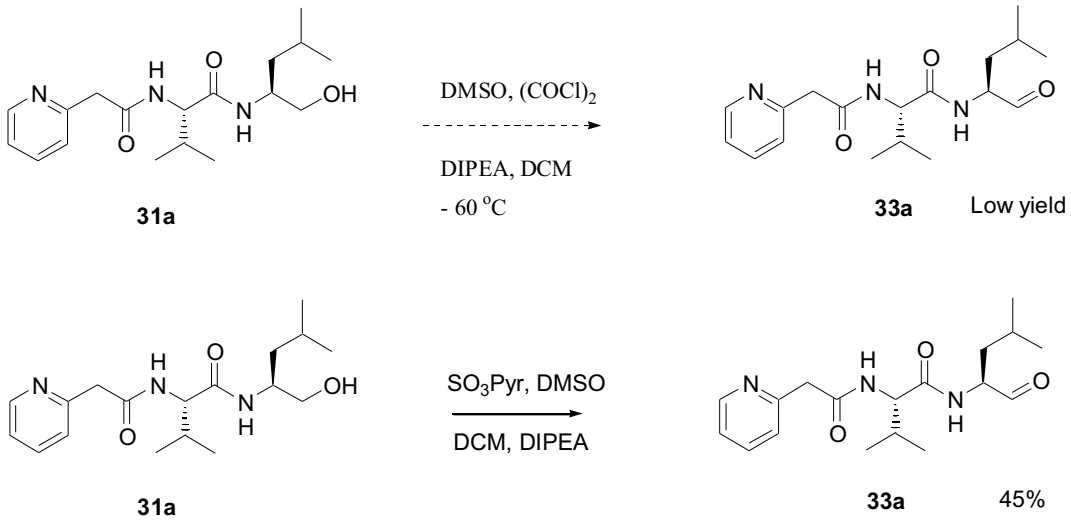

Scheme 13: Oxidation of **31a** using two conditions.

As shown in **Figure 25**, DMSO reacts with SO_3.Pyr to form a sulfonium species which contains a good-leaving group linked to the positive sulfur atom. The leaving group was then displaced with alcohol to yield an alkoxydimethylsulfonium salt followed by deprotonation by DIPEA to form the sulfur ylide. Intramolecular eliminiation leads to the formation of carbonyl compound and dimethyl sulfide.

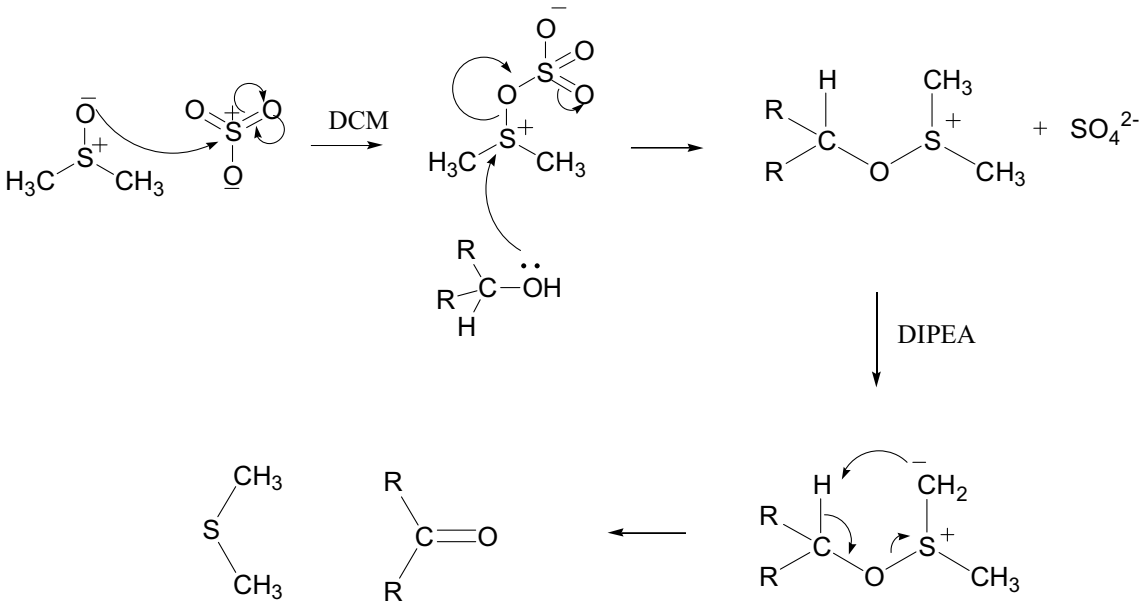

Figure 25: DMSO oxidation with sulphur trioxide pyridine as an activating reagent.

The yield of the dipeptidyl aldehydes **33a-g** and **33i** from sulfur trioxide pyridine oxidation are presented in **Table 4**.

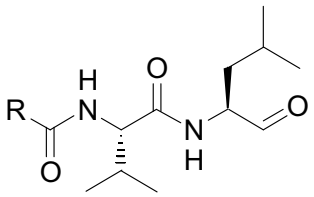

33: dipeptidyl aldehydes

No.	R	Structure	Yield
33a	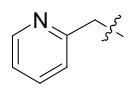	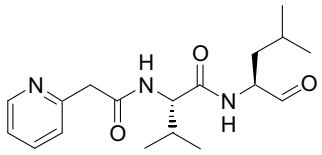	45%
33b	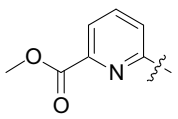	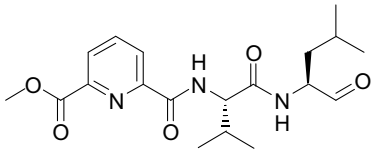	49%
33c	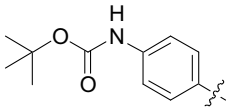	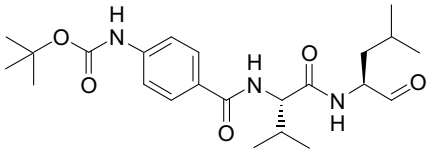	57%
33d		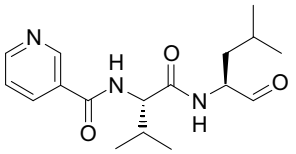	61%
33e	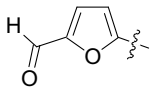	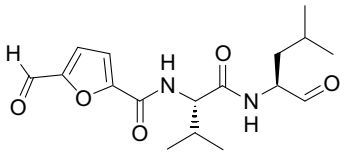	88%
33f	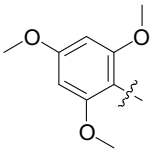	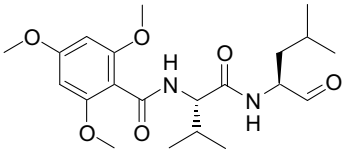	0%
33g	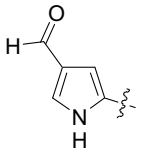	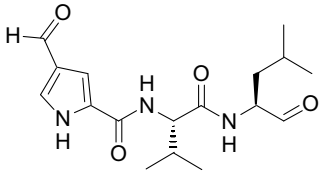	86%
33i	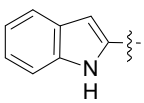	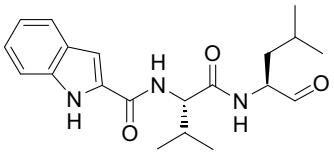	81%

Table 4: Oxidation yields results.

Chemical modification of compounds **33b** and **33c** was attempted with the aim of forming two further calpain inhibitors **34** and **35**. Base mediated hydrolysis of the ester **33b** was attempted but failed to yield the corresponding carboxylic acid **34** (**Scheme 14**).

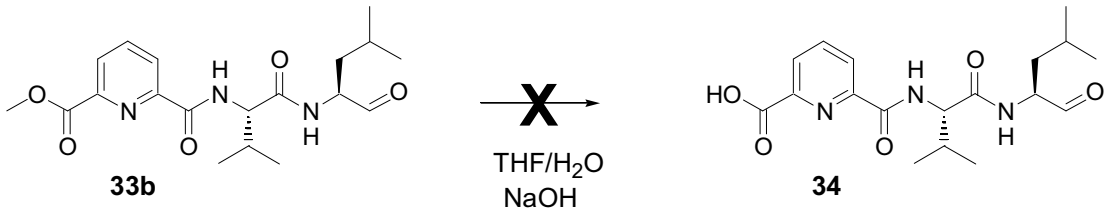

Scheme 14: Hydrolysis of methyl ester **33b**.

Hydrochloride salt **35** was synthesized *via* BOC deprotection of **33c** using 4M HCl in dioxane to give an inhibitor expected to participate in hydrogen bonding within the S_3 pocket (**Scheme 15**). The loss of the BOC group in compound **33c** was shown by the disappearance of singlet at 1.3ppm in ^{1}H NMR.

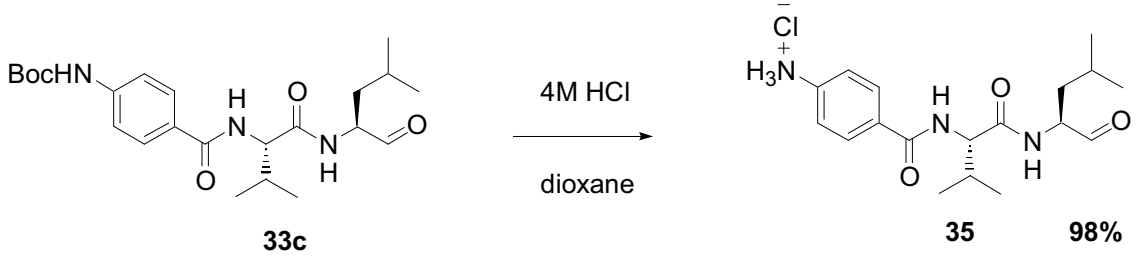

Scheme 15: BOC deprotection of **33c**.

2.2: Assay and molecular modeling results

The aldehydes **33a-e, 33g, 33i** and **35** were assayed against m-calpain using a fluorescence-based assay[65] to determine *in vitro* potency. The inhibition constant (IC_{50}) were determined (see appendix). Four compounds **33a**, **33d**, **33e** and **33g** display active inhibition and function as potent calpain inhibitors (**Figure 26**).

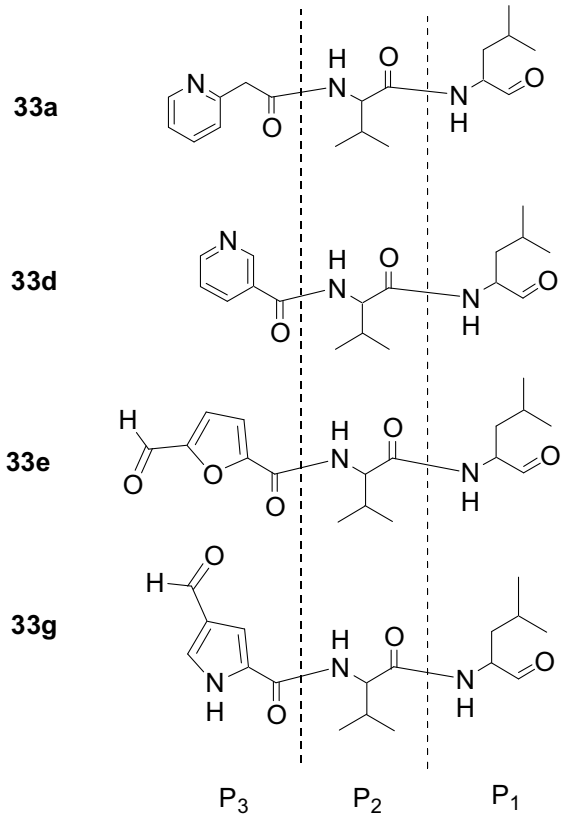

Figure 26: Structures of calpain inhibitors with nanomolar IC_{50} value.

The most potent calpain inhibitor synthesized is **33a** and its IC_{50} value is 28 nM. Based on the modeling results (**Table 5**), three hydrogen bonds (A, B, C) are formed between the backbone of ligand **33a** and Gly_{208} and Gly_{271} of calpain resulting in a bioactive β-strand conformation.[66]

Compounds	Glide score	H-bonding	Extra H-bonding	Warhead distance	IC_{50}
33a	-5.9	A,B,C	1	4.39	28 nM
33b	-5.1	A,B,C	1	4.07	3.56 μM
33c	-5.1	B,C	1	3.89	5.80 μM
33d	-4.8	A,B,C	0	3.93	86 nM
33e	-5.23	A,B,C	0	4.09	99 nM
33g	-5.2	A,B,C	1	3.77	103 nM
33i	-6.0	-	3	3.39	3.43 μM
35					27.6 μM

Table 5: Molecular docking results.

The inhibitor **33d** is potent. Its IC_{50} value is 86 nM. The activity of Val-Leu dipeptidyl aldehydes **33a**, **33d** is in accord with the docking studies that indicate valine is preferable at P_2 for binding in the S_2 pocket residues with Ala_{273}, Ser_{251} and other amino acids while leucine interacts favorably with Leu_{260} and Glu_{261} residues in S_1 pocket. Pyridin-2-yl-acetaldehyde and pyridine-3-carbaldehyde at the P_3 site are favorable for binding in the S_3 subsites.

(S)-N-((S)-1-Formyl-3-methyl-butyl)-3-methyl-2-(2-pyridin-2-yl-acetylamino)-butyrami de **33a** is a more potent inhibitor than **33d.** This may be a result of it having one more hydrogen bond between ligand **33a** and Lys_{347} in the S_3 pocket (**Figure 27**).

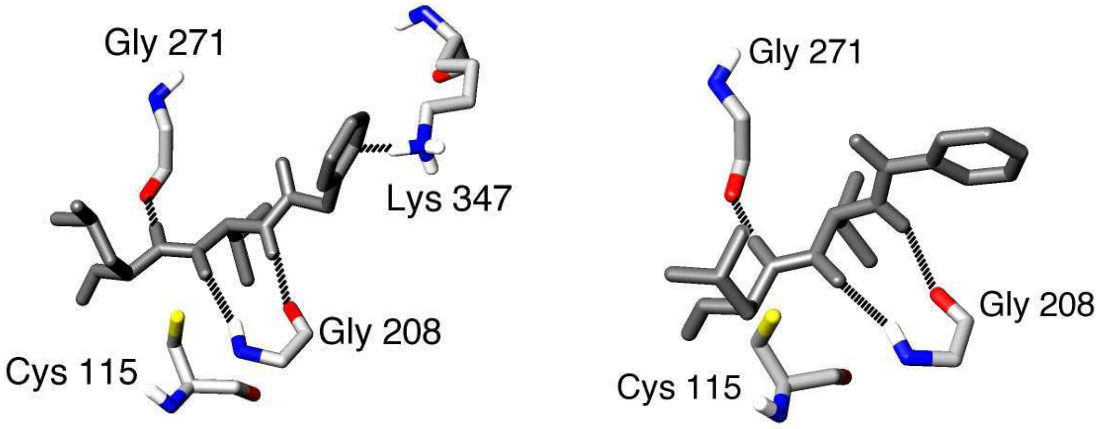

Figure 27: Molecular modeling of **33a** (left) and **33d** (right) in the S_3 binding site of m-calpain.

A comparison of **33e** (99nM) and **33g** (103nM) shows that the 5-formylfuran and 4-formylpyrrole function as both *N*-terminal capping substituents and are well accommodated in the S_3 pocket of m-calpain. This is consistent with their similar IC_{50} values. Molecular modeling shows similar binding in the active site for the both compounds. Furan **33e** binds in a standard β-stand conformation with the three defining hydrogen bonds A, B, C but no additional hydrogen bonds; whereas, **33g** binds in a standard β-strand conformation but contains an additional hydrogen bond to Lys_{347} in the S_3 pocket (**Figure 28**). Even though **33g** contains an additional hydrogen bond the increasing activity of **33g** compared to **33e** may be attributed to less steric hindrance in the S_3 pocket for **33g**.

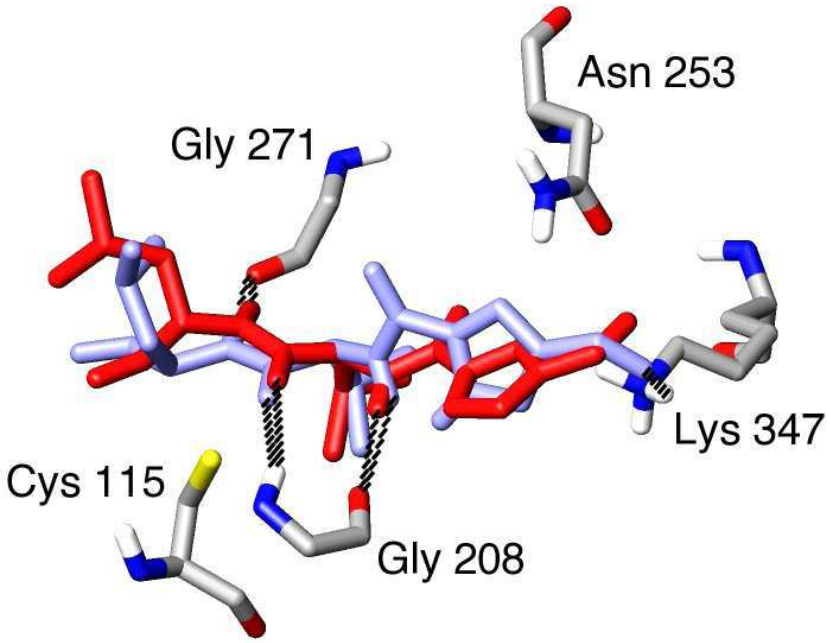

Figure 28: Molecular modeling of furan **33e** (red) and pyrrole **33g** (light blue) in the S_3 binding site of μ-calpain.

Removal of the BOC protecting group of **33c** (5.8μM) to give hydrochloride salt **35** (27.6μM) results in a dramatic decrease in potency against m-calpain. The poor inhibition of **35** indicates that the charge group is not accommodated well in the S_3 pocket. Further comparison of the protected aniline **33c** (5.8μM) and **33b** (3.65μM) reveals that Glide scores and warhead distances of these two compounds are similar; however, **33b** exhibits one more hydrogen bond than **33c** and even more importantly **33b** binds in an extended β-strand conformation (defined by three hydrogen bonds: A, B, C) resulting in more potent inhibition of m-calpain than **33c.**

Compound **33i** (3.43μM) has a good glide score (-6.0) indicating tight binding with m-calpain. The warhead is in close proximity to the active site (3.39Å); however, no hydrogen bonding occurs between the backbone of ligand **33i** and Gly_{208} and Gly_{271} of calpain. As shown in **Figure 29,** pyrrole NH and amide at P_2 position form two hydrogen bonds with Ser_{206}. The warhead carbonyl also exhibits a hydrogen bond with $His_{272.}$ Despite these three hydrogen bonds, the modeling shows that the inhibitor is not in a β-strand conformation; and compound **33i** has only moderate activity.

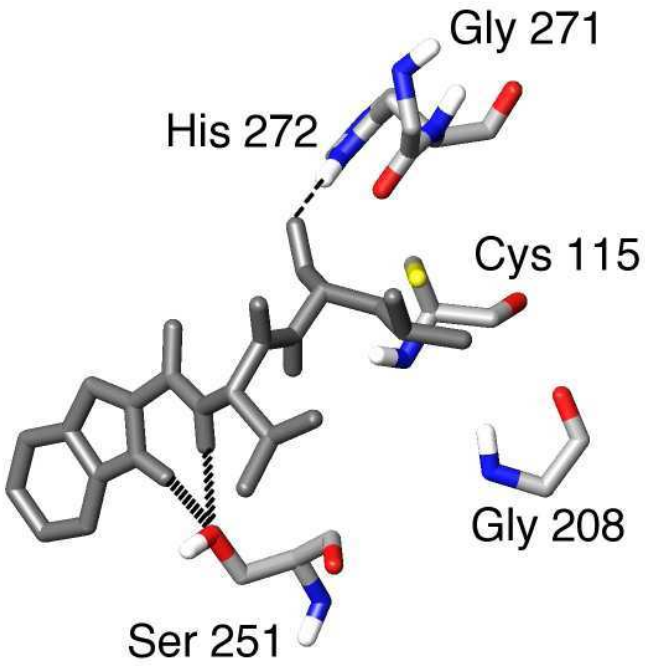

Figure 29: Molecular modeling of **33i** in the S_3 binding site of m-calpain.

2.3: Conclusion

The potent inhibitors discussed in this thesis were designed using SJA6017 as a reference. The dipeptide core of this compound has been used as a scaffold for the attachment of functional group with the ability to participate in hydrogen bonding. IC_{50} values of the inhibitors **33a-e, 33g, 33i** and **35** were determined. Four compounds (**33a, 33d, 33e**, and **33g**) gave potent nanomolar inhibition with the best compound **33a** (28nM) having an IC_{50} lower than SJA6017 (80nM). Compounds **33a** and **33d** contain a pyridine ring at the P_3 site and this can improve the corneal permeability in comparison with SJA6017 known to exhibits poor corneal permeability. Compound **33g** has a pyrrole group in place of the N-4-fluorophenylsulfonyl of SJA6017 at the P_3 position of SJA6017 and displays an active inhibition (103 nM). Furan based peptide **33e** has an IC_{50} 99 nM. Molecular modeling shows compounds **33c** (5.8 μM) and **33i** (3.43 μM) fail to bind in a β- strand conformation and these compounds exhibit only moderate activity.

2.4: References

[50] Schmuck, C.; Machon, U. *Chem. Eur. J*. **2005**, 11, 1109 – 1118.

[51] Birkett, M. A.; Giles, R. G.; Knight, D. W.; Mitchell, M. B. *J. Chem. Soc., Perkin Trans.* **1998,** 1, 2301-2305.

[52] Black, T. H.; Arrivo, S. M.; Schumm, J. S.; Knobeloch, J. M. *J. Org. Chem.* **1987**, 52, 5425-5430.

[53] Ichikawa, R.; Hata, M.; Okimoto, N.; Handa, S. O.; Tsuda. M. *Journal of Polymer Science*: *Part A: Polymer Chemistry.* **1998**, 36, 1035–1042.

[54] Han, S. Y.; Kim, Y. A. *Tetrahedron*. **2004**, 60, 2447–2467.

[55] Kappe, C. O. *Angew. Chem., Int. Ed.* **2004**, 43, 6250–6284.

[56] (a) Perreux, L.; Loupy, A.; Volatron, F. *Tetrahedron.* **2002**, 58, 2155–2162. (b) Va´zquez-Tato, M. P. *Synlett*. **1993**, 506. (c) Marrero-Terrero, A. L.; Loupy, A. *Synlett* **1996**, 245–246. (d) Seijas, J. A.; Va´zquez-Tato, M. P.; Martinez, M. M.; Nunez-Corredoira, G. *J. Chem. Res., Synop*. **1999**, 7, 420–421.

[57] Bentley, D. J.; Alexandra, M. Z.; Moody, C. J. *Organic letter.* **2006**, 8, 1975-1978.

[58] Merino, I.; Thmpson, J. D.; Millard, C. B.; Schmidt, J. J.; Pang, Y.-P. *Bioorg. Med. Chem*. **2006,** 14, 3583-3591.

[59] Pfitzner, K. E.; Moffatt, J. G.; *Journal of the American chemical society.* **1963**, 85, 3027.

[60] Albright, J. D.; Goldman, L. *Journal of the American chemical society.* **1965**, 87, 4214.

[61] Onodera, K.; Hirano, S.; Kashimura, N.; *Journal of the American chemical society.* **1965**, 87, 4651.

[62] Omura, K.; Sharma, A. K.; Swern, D. *J. Org. Chem.* **1976**, 41, 957.

[63] Mancuso, A. J.; Hunang, S.-L.; Swern, D. *J. Org. Chem.* **1978**, 43, 2480.

[64] Rarikh, J .R; Doering, W. von E. *Journal of the American chemical society.* **1967**, 89, 5505-07.

[65] Thompson, V. F.; Saldana, S.; Cong, J.; Goll, D. E. *Anal. Biochem*. **2000**, 279, 170-178.

[66] Iqbal, M.; Messina, P. A.; Freed, B.; Das, M; Chatterjee, S.; Yripathy, R.; Yao, M.; Josef, K. A.; Dembofsky, B.; Dunn, D.; Griffith, E.; Senadhi, S. E.; Biazzo, W.; Bozyczko-Coyne, D.; Meyer, S. L.; Ator, M. A.; Bihovsky, R. *Bioorg. Med. Chem. Lett.* **1997**, 7, 539-544.

Chapter 3: Experimental

3.1: General experimental methods and procedure

Analytical thin layer chromatography (TLC) was performed on plastic-backed Merck Nagel SIL G/UV254 PLATES. Visualisation was achieved by ultraviolet light and $KMnO_4$ solution or PMA. Flash chromatography was performed on 230-400 mesh Merck Silica gel 60 using the Buchi sepacore flash automated chromatography system. All eluting solvents were distilled beforehand. Proton NMR spectrometry were obtained on a Varian Inova spectrometer operating at 300 MHz. Carbon NMR spectra were obtained on a Varian Inova spectrometer operating at 75 MHz with a delay of (D1) of 1s. Spectra were obtained at 23°C. Chemical shifts are reported in parts per million (ppm) on the scale. Mass spectra were performed on a Kratos MS80 RFA mass spectrometer operating at 4000V (accelerating potential) and 70 eV (ionization energy) using a Kratos MS80 RFA spectrometer with a 250°C source. The melting points were obtained on an Electrothermal apparatus and are uncalibrated.

General procedure A1: O-(7-azabenzotriazol-1-yl)-1,1,3,3-tetramethyluronium hexafluorophosphate (HATU) mediated peptide coupling

The acid (1 equiv), ammonium salt **29** (1.1 equiv) and HATU (1.1 equiv) were dissolved in dry DMF. DIPEA was added (4 equiv) and the reaction mixture stirred at room temperature overnight. The solution was diluted with EtOAc (5:1), washed with water (2x) and brine, dried over $MgSO_4$, concentrated in vacuo and purified by column chromatography. See individual experiments for specific details.

General procedure A2: HATU mediated peptide coupling

The acid (1 equiv), ammonium salt **29** (1.5 equiv) and HATU (1.2 equiv) were dissolved in dry DMF. DIPEA was added (2.4 equiv) and the reaction mixture stirred at room temperature overnight. The solution was diluted with EtOAc (5:1), washed sequentially with HCl (1M), saturated $NaHCO_3$ and brine and dried over $MgSO_4$, filtered and concentrated in-vacuo. See individual experiments for specific details.

General procedure A3: 1-[3-(dimethylamino)propyl]-3-ethylcarbodiimide hydrochloride (EDC) mediated peptide coupling

The acid (1 equiv), ammonium salt **29** (1.5 equiv), EDC (1.2 equiv), and HOAT (1.2 equiv) and were dissolved in anhydrous DMF. DIPEA was added (2.4 equiv) immediately and the reaction mixture stirred at room temperature for 18hr. The solution was diluted with EtOAc (5:1), washed with water (2x) and brine, and dried over $MgSO_4$, concentrated in vacuo and purified by column chromatography. See individual experiments for specific details.

General procedure A4: PyBrop mediated peptide coupling

The acid (1 equiv), ammonium salt **29** (1.5 equiv) and PyBrop (1.2 equiv) were dissolved in dry DMF (1ml/60 μmmol). DIPEA was added (2.4 equiv) and the reaction mixture stirred at room temperature overnight. The solution was diluted with EtOAc (5:1), washed sequentially with HCl (1M), saturated $NaHCO_3$ and brine before being dried over $MgSO_4$, filtered and concentrated in-vacuo. See individual experiments for specific details.

General procedure B: Sulfur trioxide/pyridine complex oxidation

A solution of the alcohol in a 2:1 mixture of DMSO and DCM (0.10M) was cooled in ice. To this DIPEA (4 equiv) and a solution of SO_3.Pyr complex pre-dissolved in DMSO (1ml/60μmol) was added dropwise. The mixture was stirred in ice for 2 hr or until TLC indicated complete consumption of the starting alcohol. The reaction mixture was diluted with ethyl acetate (10:1), washed with HCl (1M, 2x), saturated $NaHCO_3$ (2x) and brine before being dried over $MgSO_4$, filtered and concentrated in vacuo. See individual experiments for specific details.

General procedure C1: Ester hydrolysis with base

To a solution of ester in THF/H_2O (3:1, 1ml/10mg) was added NaOH (2.5 equiv) and the solution was heated to 65^oC with stirring overnight. The mixture was concentrated in vacuo and the residue was partitioned between EtOAc (100ml) and water (100ml). The aqueous layer was acidified to pH 2 with 1M HCl and extracted with EtOAc (2x). The combined EtOAc layers were washed with water, brine, and dried over $MgSO_4$ and concentrated in vacuo. See individual experiments for specific details.

General procedure C2: Ester hydrolysis with base

To a solution of the ester in methanol was added NaOH (4 equiv) pre-dissolved in H_2O. The solution was heated to 65^oC with stirring overnight. The aqueous layer was acidified to pH 2 with 1M HCl and the product extracted with EtOAc (2x). The combined EtOAc layers were washed with water, brine, and dried over $MgSO_4$. The solvent was removed in vacuo. See individual experiments for specific details.

General procedure D: Esterification with $SOCl_2$ and methanol:

The carboxylic acid was suspended in methanol and cooled on ice bath. Thionyl chloride (1:10) was added dropwise and the solution was stirred at 0^oC for 3 hours before being concentrated in-vacuo. See individual experiments for specific details.

General procedure E1: N-BOC protection of an amino acid

The amino acid was dissolved in 1,4-dioxane. To this were added NaOH (4equiv) pre-dissolved in distilled water (dioxane-water 1:1), followed by di-tert-butyl dicarbonate (1.2 equiv). The mixture was stirred at room temperature overnight before being concentrated in vacuo. The residue was partitioned between ethyl acetate and 1M HCl. The aqueous phase was extracted twice with ethyl acetate and the combined organic extracts were washed with brine, dried over $MgSO_4$, filtered and concentrated in vacuo. See individual experiments for specific details.

General procedure E2: DMAP mediated N-BOC protection

Amine was dissolved in THF. Di-tert-butyl dicarbonate (5 equiv) and DMAP (1.1 equiv) were added dropwise. The mixture was stirred stirred overnight and the product isolated by concentration in vacuum. See individual experiment for specific details.

General procedure F: BOC deprotection with 4M HCl in dioxane

The N-BOC protected compound was dissolved in 4M HCl in dioxane (100mg/ml) and the solution stirred at room temperature overnight. The solvent was removed in vacuo. See individual experiment for specific details.

3.2: Experimental

6-(Methoxycarbonyl) pyridine-2-carboxylic acid (17)

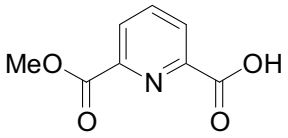

A solution of dimethyl pyridine-2, 6-dicarboxylate (11.6 g, 59.4 mmol) in methanol (300 ml) was cooled to 0^{o}C. Potassium hydroxide pellets (3.39g, 60.29 mmol) were added and the reaction mixture was stirred at 0^{o}C for 2hr and then at room temperature for 24hr. The solvent was removed under reduced pressure, and the residue was suspended in ethyl acetate (150 ml). The white potassium salt was collected by filtration and dissolved in water (100 ml). The solution was acidified to pH 3 with concentrated hydrochloric acid and extracted with chloroform (3x100 ml) and dried over $MgSO_4$. The chloroform was removed in vacuo to provide the **17** (2.90 g, 53%) as a white solid**.** m.p 146^{o}C.[67] δH ($CDCl_3$) 2.15 (1H, s, N**H**), 4.0 (3H, s, COOC**H$_3$**), 8.19 (1H, s, Ar**H**), 8.32 (2H, d, 2Ar**H**). ^{13}C NMR (75 MHz in DMSO) 52.6 (CO_2**C**H_3), 127.6 (CCH**C**H), 127.8 (C**C**HCH), 139.0 (C**C**HCH) , 147.6 (N**C**CH), 148.9 (N**C**CH), 164.8 (**C**O_2CH_3), 165.6 (CO_2H); *m/z* (ES) $[M+(H)]^+$ 182 (50%); $[M+N_a]^+$ 204 (25%).

4-(N-tert-Butoxycarbonyl) aminobenzoic acid (18)

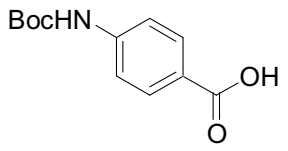

The ester **23** (920mg, 0.836mmol) was dissolved in THF (20 ml) and to this was added NaOH (4 equiv) pre-dissolved in water (20 ml). The reaction solution was stirred at 60°C overnight and concentrated to remove THF. The residue was washed with ethyl acetate (50 ml) and was acidified to pH 2 with 1M HCl. The aqueous layer was re-extracted with ethyl acetate (2 x 50 ml). The combined organic phase was washed with $NaHCO_3$, brine, and dried over $MgSO_4$. The solution was concentrated under reduced pressure to give the product **18** as a white solid (768mg, 88.5%). mp 191-192 °C; δH ($CDCl_3$) 1.50-1.56 (9H, m, (C**H**$_3$)$_3$), 6.67 (s, N**H**), 7.41 (2H, d, 2Ar**H**), 7.95 (2H, d, 2Ar**H**).

4-Formyl-1H-pyrrole-2-carboxylic acid (19)

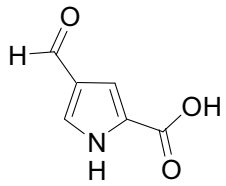

The methyl ester **25** (2.17g, 13mmol) was hydrolysed using general procedure C2 to afford **19** as yellow solid (1.53g, 85%). mp 234-236°C. ^{1}H NMR (300 MHz in $(CD_3)_2SO$) 7.07 (1H, d, Ar**H**), 7.77 (1H, d, Ar**H**), 9.74 (1H, s, C**H**O), 12.53 (1H, s, N**H** Pyrrole), 12.85 (1H, s, CO_2**H**); ^{13}C NMR (75 MHz in DMSO). 112.5 (**C**HCNH), 125.6 (**C**HNH), 126.5 (CH**C**CHO), 130.8 (CH**C**CO_2H), 161.5 (CCO_2H), 185.8 (**C**HO),[68] LRMS (ES) 140.0 (MH^+). $C_6H_5NO_3$ requires 140.0.

Pyridine-2, 6-dicarboxylic acid dimethyl ester (21)

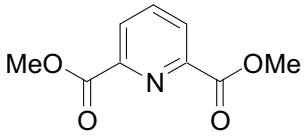

Pyridine-2, 6-dicarboxylic acid (10g, 59.8mmol) was treated using general procedure D to provide dimethyl pyridine-2, 6-dicarboxylate as a white solid (11.72g, 100%). δH ($CDCl_3$) 2.11 (1H, s, N**H**), 4.0 (6H, s, 2 COOC**H$_3$**), 7.98 (1H, s, Ar**H**), 8.27 (2H, d, 2Ar**H**). m.p. 117 – 119^{o}C; (Found: C, 55.45; H, 4.60; N, 7.18%. $C_9H_9O_4N$ requires C, 55.43; H, 4.65: N, 7.18%).[69] The crude product was used in the following step without further purification.

4-tert-Butoxycarbonylamino-benzoic acid methyl ester (23)

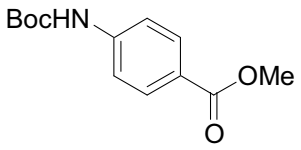

4-Amino-benzoic acid methyl ester **22** (2g, 13.23mmol) was reacted with di-tert-butyl dicarbonate using general procedure E2. The crude product was purified with flash column chromatography over silica gel with ethyl acetate/ petroleum ether (gradient 1/3 to 1/4) as eluent to give compound **23** as a white solid (2.4g, 72%). R_f= 0.30; δH ($CDCl_3$) 1.38-1.42 (12H, d, (C**H$_3$**)$_3$), 3.91 (3H, s, COOC**H$_3$**), 7.25 (2H, d, 2Ar**H**), 8.05 (2H, d, 2 Ar**H**). *m/z* (ES) $[M+(H)]^+$ 253 (60%); $[M+N_a]^+$ 272 (25%).

[(S)-1-((S)-1-Hydroxymethyl-3-methyl-butylcarbamoyl)-2-methyl-propyl]-carbamic acid tert-butyl ester (28)

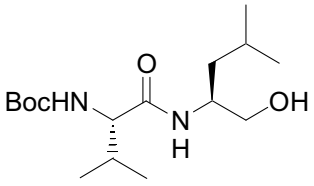

BOC Val-OH **26** (15.93g, 0.0734mol) was reacted with L-Leucinol **27** using the general procedure A2. The crude product was purified with flash column chromatography over silica gel using ethyl acetate - petroleum ether (1:1) as eluent to give **28** as a white solid (12.19g, 53%). R_f=0.4; δH (CD_3OD) 0.88-0.98 (12H, m, ($C\mathbf{H_3}$)$_4$), 1.30-1.40 (9H, m, $C(C\mathbf{H_3})_3$), 1.30–1.50 (2H, m, $CHC\mathbf{H_2}CH(CH_3)_2$), 1.70 (1H, m, $CHCH_2C\mathbf{H}(CH_3)_2$), 1.98 (1H, m, $CHC\mathbf{H}(CH_3)_2$), 3.55 (2H, t, $C\mathbf{H_2}OH$), 3.80 (1H, d, $C\mathbf{H}CH(CH_3)_2$), 4.0 (1H, m, $C\mathbf{H}CH_2CH(CH_3)_2$). ^{13}C NMR (75 MHz, $CDCl_3$) 18.0 ($\mathbf{C}H_3$), 19.2 ($\mathbf{C}H_3$), 22.0 ($CH_2\mathbf{C}H(CH_3)_2$), 23.0 ($\mathbf{C}H_3$), 24.7 ($\mathbf{C}H_3$), 28.2 ($C(\mathbf{C}H_3)_3$), 30.4 ($\mathbf{C}H(CH_3)_2$), 39.8 ($\mathbf{C}H_2CH(CH_3)_2$), 49.9 ($\mathbf{C}HCH_2OH$), 60.5 ($\mathbf{C}HCH(CH_3)_2$), 65.5 ($\mathbf{C}H_2OH$), 80.9 ($\mathbf{C}(CH_3)_3$), 156.1 (Boc**C**O), 172.2 (**C**ONH). HRMS (ES+) calcd. for $C_{16}H_{33}N_2O_4$ ($M+H^+$) 317.2240 found 317.2249.

(S)-2-Amino-N-((S)-1-hydroxymethyl-3-methyl-butyl)-3-methyl-butyramide (29)

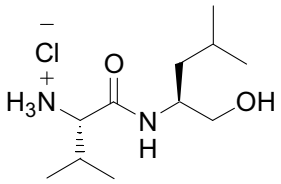

BOC-Val-Leu-OH **28** (12.19g) was reacted using general procedure F to afford **29** as a white solid (10.2g, 100%). mp 82-86^{o}C. This product was used without further purification. δH (CD_3OD) 0.90 (3H, d, $C\mathbf{H_3}$), 0.94 (3H, d, J 6.3, $C\mathbf{H_3}$), 1.03 (3H, d, J 6.8, $C\mathbf{H_3}$), 1.06 (3H, d, J 6.8, $C\mathbf{H_3}$), 1.30–1.40 (2H, m, $CHC\mathbf{H_2}CH(CH_3)_2$), 1.65 (1H, m, $CHCH_2C\mathbf{H}(CH_3)_2$), 2.2 (1H, m, $CHC\mathbf{H}(CH_3)_2$), 3.5 (2H, t, $C\mathbf{H_2}OH$), 3.7 (1H, d, $C\mathbf{H}CH(CH_3)_2$), 4.0 (1H, m, $C\mathbf{H}CH_2CH(CH_3)_2$). ^{13}C NMR (75 MHz in DMSO) 17.9 ($\mathbf{C}H_3$), 18.2 ($\mathbf{C}H_3$), 21.9 ($CH_2\mathbf{C}H(CH_3)_2$), 23.3 ($\mathbf{C}H_3$), 23.9 ($\mathbf{C}H_3$), 29.7 ($\mathbf{C}H(CH_3)_2$), 49.2 ($\mathbf{C}HCH_2OH$), 57.3 ($\mathbf{C}HCH(CH_3)_2$), 63.4 ($\mathbf{C}H_2OH$), 167.1 (**C**ONH). (Found C, 48.67; H,

9.81; N, 10.50% $C_{11}H_{25}ClN_2O_2.H_2O$ requires C, 48.79; H, 10.05; N, 10.34%). HRMS (ES+) calcd for $C_{11}H_{25}N_2O_2$ $[M+H]^+$ 217.1916 found 217.1924.

(S)-N-((S)-1-Hydroxymethyl-3-methyl-butyl)-3-methyl-2-(2-pyridin-2-yl-acetylamio) -butyramide (31a)

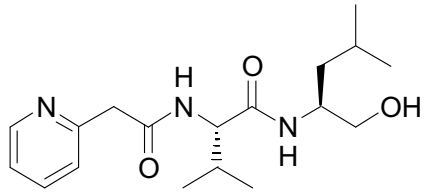

2-Pyridylacetic acid **30a** (0.344 g, 1.978 mmol) was reacted with ammonium salt **29** using the general procedure A4. The crude product was purified with flash column chromatography over silica gel using MeOH-DCM (5%) as eluent to give **31a** as a white solid (404mg, 61%). R_f=0.4; δH (CD_3OD) 0.83 (3H, d, C**H**$_3$), 0.85 (3H, d, C**H**$_3$), 0.86 (6H, d, (C**H**$_3$)$_2$), 1.33 (2H, m, CHC**H**$_2$CH(CH$_3$)$_2$), 1.61 (1H, m, CHCH$_2$C**H**(CH$_3$)$_2$), 2.17 (1H, m, CHC**H**(CH$_3$)$_2$), 3.43 (2H, t, C**H**$_2$OH), 3.77 (1H, d, C**H**CH(CH$_3$)$_2$), 3.98 (1H, m, C**H**CH$_2$CH(CH$_3$)$_2$), 4.18 (2H, d, C**H**$_2$CO), 7.23 (1H, d, N**H**), 7.37 (1H, d, N**H**), 7.78 (2H, m, 2Ar**H**), 8.23(2H, s, 2Ar**H**). ^{13}C NMR (75 MHz, CD_3OD) 17.1 (**C**H$_3$), 18.4 (**C**H$_3$), 20.8 (**C**H$_3$), 22.6 (**C**H$_3$), 24.5 (CHCH$_2$**C**H(CH$_3$)$_2$), 29.3 (CH**C**H(CH$_3$)$_2$), 30.3 ((**C**H(CH$_3$)$_2$), 39.7 (CH**C**H$_2$CH(CH$_3$)$_2$), 47.8 (**C**HCH$_2$OH), 48.6 (**C**HCH$_2$CH(CH$_3$)$_2$), 59.3 (**C**HCH(CH$_3$)$_2$), 64.2 (**C**H$_2$OH), 122.2 (NCH**C**HCHCH), 124.1 (NCHCH**C**HCH), 137.4 (NCHCHCH**C**H), 148.5 (N**C**HCH), 157.1 (**C**ONH), 170.3 (**C**ONH); *m/z* (ES) $[M+(H)]^+$ 337 (45%); $[M+N_a]^+$ 358 (25%).

6-[(S)-1-((S)-1-Hydroxymethyl-3-methyl-butylcarbamoyl)-2-methyl-propylcarbamoyl]-pyridine-2-carboxylic acid methyl ester (31b)

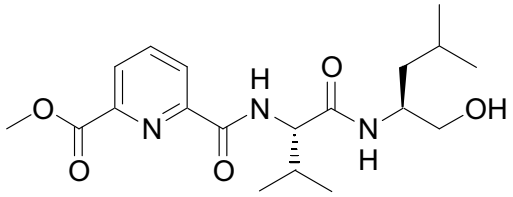

Pyridine carboxylic acid **17** (500 mg, 2.77 mmol), ammonium salt **29** (701.46 mg, 2.77 mol), DIPEA (1.1 ml, 6.66 mmol), HOAT (453 mg, 3.33 mmol) and HATU (1.16 g, 3.05 mmol) were dissolved in DMF. The solution turned yellow and was stirred overnight. The mixture was diluted with ethyl acetate, and the organic layer washed with aqueous HCl, (1M) saturated aqueous $NaHCO_3$ and brine, and dried over $MgSO_4$. The solvent was removed in vacuo. The crude product was purified by flash column chromatography over silica gel using ethyl acetate - petroleum ether (gradient 1:1 to 2:1) as eluent to give **31b** as a white solid (874 mg, 83.2%). R_f= 0.45; δH (CD_3OD) 0.90 (3H, d, C**H**$_3$), 0.94 (3H, d, J 6.3, C**H**$_3$), 1.03 (3H, d, J 6.8, C**H**$_3$), 1.06 (3H, d, J 6.8, C**H**$_3$), 1.35-1.45 (2H, m, CHC**H**$_2$CH(CH_3)$_2$), 1.70 (1H, m, CHCH_2C**H**(CH_3)$_2$), 2.17 (1H, m, CHC**H**(CH_3)$_2$), 3.51 (2H, t, C**H**$_2$OH), 3.77 (1H, d, C**H**CH(CH_3)$_2$), 4.02 (3H, m, COOC**H**$_3$) 4.38 (1H, m, C**H**CH_2CH(CH_3)$_2$), 7.95 (1H, d, N**H**), 8.19 (1H, t, Ar**H**), 8.30 (1H, t, Ar**H**), 9.18 (1H, d, N**H**). ^{13}C NMR (75 MHz, CD_3OD) 18.3 (**C**H_3), 19.6 (**C**H_3), 22.1, 22.8 (**C**H_3), 24.8 (CHCH_2**C**H(CH_3)$_2$), 30.5 (CH**C**H(CH_3)$_2$), 30.9 (**C**H(CH_3)$_2$), 39.8 (CH**C**H_2CH(CH_3)$_2$), 50.3 (**C**HCH_2OH), 52.9 , 59.7 (**C**HCH(CH_3)$_2$), 65.6 (**C**H_2OH), 76.5 (O**C**H_3), 77.0, 77.4, 125.7 (CH**C**HCH), 127.5 (**C**HCHCH), 138.6 (CHCH**C**H), 146.7 (CH**C**CO), 149.3 (CH**C**CO), 164.2 (**C**ONH), 171.5 (**C**ONH), 207.0 (**C**ONH); *m/z* (ES) $[M+(H)]^+$ 381 (30%); $[M+N_a]^+$ 402 (25%).

{4-[(S)-1-((S)-1-Hydroxymethyl-3-methyl-butylcarbamoyl)-2-methyl-propylcarbamoyl]-phenyl}-carbamic acid tert-butyl ester (31c)

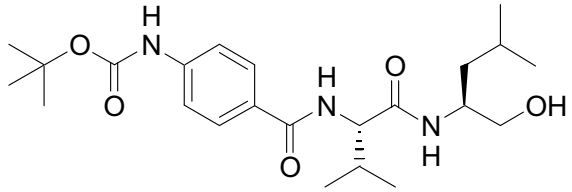

The aminobenzoic acid **18** (768 mg, 3.24 mmol) and ammonium salt **29** were coupled by the general procedure A1. The crude product was purified by flash column chromatography over silica gel using ethyl acetate - petroleum ether (1:1) as eluent to give **31c** as a white solid (916mg, 65%). R_f=0.34; δH (CD_3OD) 0.86-0.92 (6H, m, ($C\mathbf{H_3}$)$_2$), 1.03 (6H, d, ($C\mathbf{H_3}$)$_2$), 1.40 (2H, m, CHC$\mathbf{H_2}$CH(CH_3)$_2$), 1.50 (9H, s, ($C\mathbf{H_3}$)$_3$) 2.17-2.21 (1H, m, $CHCH_2C\mathbf{H}(CH_3)_2$), 3.30 (1H, m, CHC**H**(CH_3)$_2$), 3.45 (2H, m, C$\mathbf{H_2}$OH), 4.25 (1H, t, C**H**CH(CH_3)$_2$), 7.50 (2H, d, 2Ar**H**), 7.75 (2H, d, 2Ar**H**), 7.79 (1H, d, N**H** Val), 8.01 (1H, d, N**H**, Leu), 9.17 (1H, s, N**H**). ^{13}C NMR (75 MHz, CD_3OD) 13.4 (CH**C**H_3), 18.2 (CH**C**H_3), 18.8 (CH**C**H_3), 19.8 (C**C**H_3), 21.2 (C**C**H_3), 22.7 (C**C**H_3), 24.8 ($CHCH_2$**C**H(CH_3)$_2$), 27.6 (CH**C**H(CH_3)$_2$), 30.8 (CH**C**H(CH_3)$_2$), 40.0 (CH**C**H_2CH(CH_3)$_2$), 48.8 (**C**H_2OH), 49.7 (**C**(CH_3)$_3$), 60.2 (**C**HCH_2CH(CH_3)$_2$), 64.6 (**C**HCH(CH_3)$_2$), 117.7 (**C**HCHC), 127.8 (**C**HCHC), 128.3 (CH**C**HC), 143.2 (CHCH**C**), 153.5 (Boc**C**O), 168.7 (**C**ONH), 172.0 (**C**ONH). *m/z* (ES) $[M+(H)]^+$ 436 (50%); $[M+N_a]^+$ 457 (30%).

N-[(S)-1-((S)-1-Hydroxymethyl-3-methyl-butylcarbamoyl)-2-methyl-propyl]-nicotinamide (31d)

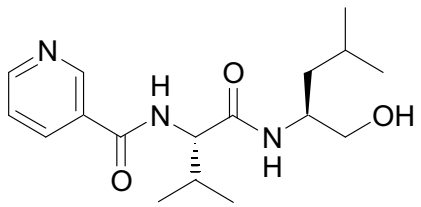

Nicotinic acid **30d** (253.3mg, 2.057mmol) was reacted with ammonium salt **29** using general procedure A3 to give **31d** as a white solid (430mg, 68%). mp 136-138°C; R_f=0.51; δH (CD_3OD) 0.87 (3H, d, C**H**$_3$), 0.89 (3H, d, C**H**$_3$), 1.02 (6H, d, (C**H**$_3$)$_2$), 1.35–1.45 (2H, m, CHC**H**$_2$CH(CH_3)$_2$), 1.63 (1H, m, CHCH_2C**H**(CH_3)$_2$), 2.19 (1H, m, CHC**H**(CH_3)$_2$), 3.47 (2H, t, C**H**$_2$OH), 4.02 (1H, m, C**H**CH(CH_3)$_2$), 4.35 (1H, d, C**H**CH_2CH(CH_3)$_2$), 7.51 (1H, t, Ar**H**), 8.22 (1H, d, N**H**), 8.85 (1H, d, N**H**), 8.96 (1H, s, Ar**H**). ^{13}C NMR (75 MHz, CD_3OD) 13.1 (**C**H_3), 17.8 (**C**H_3), 20.8 (**C**H_3), 22.4 (**C**H_3), 24.5 (CHCH_2**C**H(CH_3)$_2$), 30.3 (CH**C**H(CH_3)$_2$), 39.7 (CH**C**H_2CH(CH_3)$_2$), 51.4 (**C**HCH_2CH(CH_3)$_2$), 60.1 (**C**HCH(CH_3)$_2$), 64.2 (**C**H_2OH), 123.7 (CH**C**HCHC), 130.6 (CHCH**C**HC), 135.8 (CHCHCH**C**), 147.9 (CH**C**HN), 151.3 (C**C**HN), 166.6 (**C**ONH), 171.9 (**C**ONH); *m/z* (ES) $[M+(H)]^+$ 323 (55%); $[M+N_a]^+$ 344 (30%).

5-Formyl-furan-2-carboxylic acid {1-[(S)-1-((S)-hydroxymethyl)-3-methyl-butyl carbamoyl]-2-methylpropyl}-amide (31e)

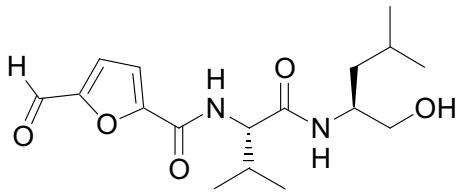

5-Formyl-furan-2-carboxylic acid **30e** (277.1mg, 1.98mmol) was reacted with ammonium salt **29** using the general procedure A3. The crude product was purified with flash column chromatography over silica gel with ethyl acetate - petroleum ether (4:1) as eluent to give **31e** as a white solid (198 mg, 31%). R_f=0.21; ν_{max} (KBr) 1638 (C=ONH), 1038 (C-OH); δH (DMSO) 0.77-0.86 (12H, m, (C**H**$_3$)$_4$), 1.25 (2H, m, CHC**H**$_2$CH(CH_3)$_2$), 1.58 (1H, m, CHCH_2C**H**(CH_3)$_2$), 2.03 (1H, m, CHC**H**(CH_3)$_2$), 3.20 (1H, m, C**H**$_2$OH), 3.29 (1H, m, C**H**$_2$OH), 3.79 (1H, m, C**H**CH(CH_3)$_2$), 4.0 (1H, m, C**H**CH_2CH(CH_3)$_2$). 7.40 (1H, m, Ar**H**), 7.58 (1H, d, Ar**H**), 7.80 (1H, d, N**H**), 8.39(H, d, N**H**), 9.67 (1H, s, C**H**O).

^{13}C NMR (75 MHz, CDCl3) 18.9 (**C**H_3), 19.1 (**C**H_3), 22.4 (**C**H_3), 22.8 (**C**H_3), 24.9 (CH**C**H(CH_3)$_2$), 40.0 (CH**C**H_2CH(CH_3)$_2$), 48.6 (**C**HCH_2CH(CH_3)$_2$), 58.4 (**C**HCH(CH_3)$_2$), 64.8 (**C**H_2OH), 110.7 (**C**HCCHO), 122.0 (**C**HCCO), 132.3 (CH**C**CHO), 133.6 (CH**C**CO), 159.5 (**C**ONH), 171.0 (**C**ONH), 181.0 (**C**HO). HRMS (ES+) calcd for $C_{17}H_{27}N_3O_4$ ($M+H^+$) 338.2080 found 338.2086.

N-[1-((S)-1-Hydroxymethyl-3-methyl-butylcarbamoyl)-2-methyl-propyl]-2,4,6-trimethoxy-benzamide (31f)

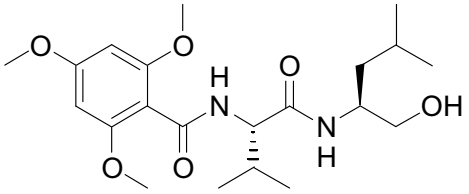

2,4,6-Trimethoxy-benzoic acid **30f** (420mg, 1.978mmol), was reacted with ammonium salt **29** using general procedure A3. The crude product was purified with flash column chromatography over silica gel using MeOH/DCM (5%) to give **31f** as a white solid (613 mg, 76%). mp 188-190^{o}C. R_f=0.25; δH (DMSO) 0.90 (6H, m, (C**H$_3$**)$_2$), 1.07 (6H, m, (C**H$_3$**)$_2$), 1.41 (2H, m, CHC**H$_2$**CH(CH_3)$_2$), 1.70 (1H, m, CHCH_2C**H**(CH_3)$_2$), 2.21 (1H, m, CHC**H**(CH_3)$_2$), 3.50 (2H, t, C**H$_2$**OH), 3.85 (3H, s, OC**H$_3$**), 3.92 (6H, s, O(C**H$_3$**)$_2$), 4.02 (1H, m, C**H**CH_2CH(CH_3)$_2$), 4.37 (1H, d, C**H**CH(CH_3)$_2$), 7.23 (2H, s, 2Ar**H**), 8.45 (1H, d, N**H**), 8.75(1H, d, N**H**). ^{13}C NMR (75 MHz, CD3OD) 18.2 (**C**H_3), 18.7 (**C**H_3), 21.1 (**C**H_3), 22.6 (**C**H_3), 24.7 (CH**C**H(CH_3)$_2$), 40.0 (CH**C**H_2CH(CH_3)$_2$), 48.1 (**C**HCH_2CH(CH_3)$_2$), 49.7 (**C**HCH(CH_3)$_2$), 55.6 (**C**H_3O), 60.0 (**C**H_3O), 60.4 (**C**H_3O), 64.4 (**C**H_2OH), 97.0 (**C**HCCH) , 105.0 (CHC**C**H), 129.6 (CH_3O**C**), 153.3 (CH_3O**C**), 159.6 (CH_3O**C**), 168.5 (**C**ONH), 172.6, (**C**ONH). (Found C, 61.65; H, 8.44; N, 6.82% $C_{21}H_{34}N_2O_6$ requires C, 61.44; H, 8.35; N, 6.82%). *m/z* (ES) $[M+(H)]^+$ 412 (50%); $[M+N_a]^+$ 432 (25%).

4-Formyl-1H-pyrrole-2-carboxylic acid {1-[(S)-1-((S)-hydroxymethyl)-3-methyl-butyl-carbamoyl]-2-methyl-propyl}-amide (31g)

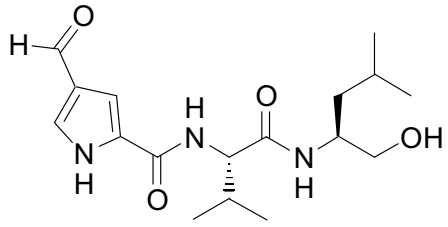

4-Formyl-1H-pyrrole-2-carboxylic acid **19** (275mg, 1.98 mmol) was reacted with ammonium salt **29** using general procedure A3. The crude product was purified with flash column chromatography over silica gel using ethyl acetate - petroleum ether (4:1) as eluent to give **31g** as a white solid (236 mg, 36%). mp 112-115^{o}C; R_f=0.30; HRMS (ES+) calcd for $C_{17}H_{27}N_3O_4$ ($M+H^+$) 338.2080 found 338.2066; ν_{max} (KBr) 1624 (C=ONH), 1038 (C-OH); δH (DMSO) 0.85-0.90 (12H, m, (C**H**$_3$)$_4$), 1.27-1.31 (2H, m, CHC**H**$_2$CH(CH$_3$)$_2$), 1.60 (1H, m, CHCH$_2$C**H**(CH$_3$)$_2$), 2.09 (1H, m, CHC**H**(CH$_3$)$_2$), 3.35 (2H, t, C**H**$_2$OH), 3.82 (1H, m, C**H**CH(CH$_3$)$_2$), 4.22 (1H, t, C**H**CH$_2$CH(CH$_3$)$_2$), 7.41 (1H, s, Ar**H**), 7.65 (1H, d, N**H**), 7.70 (1H, s, Ar**H**), 8.14 (1H, d, N**H**), 9.74 (1H, s, C**H**O), 12.33 (1H, s, N**H,** Pyrrole) ^{13}C NMR (75 MHz, (DMSO) 19.5 (**C**H$_3$), 20.0 (**C**H$_3$), 22.5 (**C**H$_3$), 24.1 (**C**H$_3$), 24.8 (CHCH$_2$**C**H(CH$_3$)$_2$), 32.2 (CH**C**H(CH$_3$)$_2$), 41.1 (CH**C**H$_2$CH(CH$_3$)$_2$), 49.4 (**C**H$_2$OH), 59.3 (**C**HCH$_2$CH(CH$_3$)$_2$), 64.6 (**C**HCH(CH$_3$)$_2$), 109.5 (**C**HCH), 127.1, (**C**HCCHO), 129.2 (**C**CONH), 130.9 (**C**N), 160.6 (**C**ONH), 171.3 (**C**ONH), 186.6 (C**C**HO); *m/z* (ES) ($[M+(H)]^+$, 338 (10%), (Found C, 59.12; H, 8.01; N, 12.04% $C_{17}H_{27}N_3O_4$.0.67H_2O requires C, 58.94; H, 8.15; N, 12.13%). ($[M+(Na)]^+$, 360 (100%).

1H-Indole-2-carboxylic acid [(S)-1-((S)-1-hydroxymethyl-3-methyl-butylcarbamoyl)-2-methyl-propyl]-amide (31i)

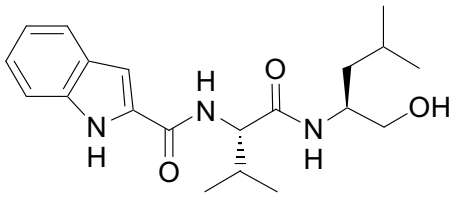

Indole-2-carboxylic acid **30i** (319mg, 1.98 mmol) was reacted with ammonium salt **29** using general procedure A3. The crude product was purified by flash column chromatography over silica gel using ethyl acetate - petroleum ether (1:1) as eluent to give **31i** as a white solid (497mg, 70%). mp 61-63^{o}C; R_f=0.17; δH (CD_3OD) 0.89-0.91 (6H, m, (C**H**$_3$)$_2$), 1.06-1.08 (6H, m, (C**H**$_3$)$_2$, 1.41 (2H, m, CHC**H**$_2$CH(CH_3)$_2$), 1.65 (1H, m, $CHCH_2$C**H**(CH_3)$_2$), 2.20 (1H, m, CHC**H**(CH_3)$_2$), 3.56 (2H, t, C**H**$_2$OH), 4.06 (1H, m, C**H**$CH_2CH(CH_3)_2$), 4.41 (1H, m, C**H**$CH(CH_3)_2$), 7.09 (2H, t, 2Ar**H**), 7.21 (2H, t, 2Ar**H**), 7.43 (1H, d, N**H**), 7.65 (1H, d, N**H**), 8.08 (1H, d, N**H**). ^{13}C NMR (75 MHz, CDCl3) 19.5 (**C**H_3), 20.0 (**C**H_3), 22.5 (**C**H_3), 24.1 (**C**H_3), 24.9 (CH**C**$H(CH_3)_2$), 40.2 (CH**C**$H_2CH(CH_3)_2$), 49.4 (**C**$HCH_2CH(CH_3)_2$), 59.3 (**C**$HCH(CH_3)_2$), 64.5 (**C**H_2OH), 104.3 (NHCCH**C**H), 112.2 (NHCCHCH**C**H), 120.4 (C**C**HCH), 124.1 (NHC**C**H), 127.7 (NHC**C**), 132.0 (NH**C**C), 137.2 (NHC**C**H), 161.5 (**C**ONH), 171.3 (**C**ONH). (Found C, 66.64; H, 8.03; N, 11.51% $C_{20}H_{29}N_3O_3$ requires C, 66.83; H, 8.13; N, 11.69%). HRMS (E+S) calc for $C_{17}H_{25}N_3O_3$ ([M+H]$^+$) 360.2287 found 360.2271.

(S)-N-((S)-1-Formyl-3-methyl-butyl)-3-methyl-2-(2-pyridin-2-yl-acetylamino)-butyramide (33a)

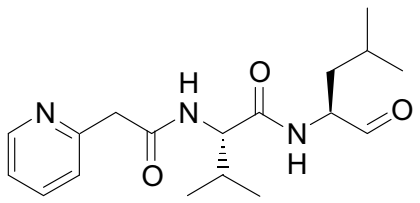

Alcohol **31a** (170 mg, 0.5 mmol) was oxidised using general procedure B. The crude product was purified by flash column chromatography over silica gel using MeOH - DCM (5%) as eluent to give **33a** as a white solid (84 mg, 45%). mp 116-118^{o}C; R_f= 0.34; δH (DMSO) 0.82-0.88 (12H, m, (C**H**$_3$)$_4$), 1.51-1.60 (3H, m, CHC**H**$_2$CH(CH$_3$)$_2$ and CHCH$_2$C**H**(CH$_3$)$_2$), 2.04 (1H, m, CHC**H**(CH$_3$)$_2$), 3.70 (2H, s, C**H**$_2$CO), 4.12 (1H, m, C**H**CH(CH$_3$)$_2$), 4.21 (2H, t, C**H**CH$_2$CH(CH$_3$)$_2$), 7.21 (1H, t, Ar**H**), 7.25 (1H, d, N**H**), 7.75 (1H, t, Ar**H**), 8.21(2H, d, N**H**), 8.43 (2H, t, 2Ar**H**), 9.38 (1H, s, C**H**O). ^{13}C NMR (75 MHz, CD$_3$OD) 18.0 (**C**H$_3$), 19.2 (**C**H$_3$), 21.3 (**C**H$_3$), 23.1 (**C**H$_3$), 24.0 (CHCH$_2$**C**H(CH$_3$)$_2$), 30.4 (CH**C**H(CH$_3$)$_2$), 36.2 (CH**C**H$_2$CH(CH$_3$)$_2$), 39.6 (**C**H$_2$CO), 56.7 (**C**HCH$_2$CH(CH$_3$)$_2$), 57.6 (**C**HCH(CH$_3$)$_2$), 121.7 (CH**C**HCHCH), 123.6 (CHCH**C**HCH), 136.5 (CHCHCH**C**H), 147.6 (N**C**HCH), 156.5 (N**C**CH), 169.1 (**C**ONH), 171.1 (**C**ONH), 201.1 (CH**C**HO). *m/z* (ES) [M+(H)]$^+$ 334 (50%).

6-[(S)-1-((S)-1-Formyl-3-methyl-butylcarbamoyl)-2-methyl-propylcarbamoyl]-pyridine-2-carboxylic acid methyl ester (33b)

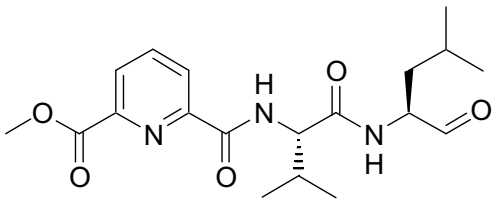

Alcohol **31b** (400 mg, 1.06 mmol) was oxidised using general procedure B. The crude product was purified by flash column chromatography over silica gel using ethyl acetate - petroleum ether (1:2 - 1:1) as eluent to give **33b** as a white solid (193mg, 49%). R_f=0.43; δH (DMSO) 0.82-0.95 (12H, m, (C**H**$_3$)$_4$), 1.30–1.40 (2H, m, CHC**H**$_2$CH(CH$_3$)$_2$), 1.60 (1H, m, CHCH$_2$C**H**(CH$_3$)$_2$), 2.12 (1H, m, CHC**H**(CH$_3$)$_2$), 3.92 (3 H, s, COOC**H**$_3$), 4.20 (1H, m, C**H**CH(CH$_3$)$_2$), 4.52 (1H, m, C**H**CH$_2$CH(CH$_3$)$_2$), 8.23-8.28 (3H, m, Ar**H**), 8.42 (1H, d, N**H** Val), 8.67 (1H, d, N**H** Leu), 9.43 (1H, s, C**H**O). ^{13}C NMR (75 MHz, CD$_3$OD) 18.3 (**C**H$_3$), 19.4 (**C**H$_3$), 22.1 (**C**H$_3$), 22.8 (**C**H$_3$), 24.8 (CHCH$_2$**C**H(CH$_3$)$_2$), 30.5

(CH**C**H(CH$_3$)$_2$), 36.9 (CH**C**H$_2$CH(CH$_3$)$_2$), 50.3 (**C**H$_3$O), 52.9 (**C**HCH$_2$CH(CH$_3$)$_2$), 59.6 (**C**HCH(CH$_3$)$_2$), 125.4 (CH**C**HCH), 127.5 (**C**HCHCH), 138.6 (CHCH**C**H), 146.7 (**C**N), 149.3 (**C**N), 162.6 (**C**ONH), 164.4 (**C**ONH), 169.3 (**C**OOCH$_3$) 201.0 (CH**C**HO); *m/z* (ES) [M+(H)]$^+$ 379 (20%); [M+N$_a$]$^+$ 395 (15%).

{4-[(S)-1-((S)-1-Formyl-3-methyl-butylcarbamoyl)-2-methyl-propylcarbamoyl]-pheyl}-carbamic acid tert-butyl ester (33c)

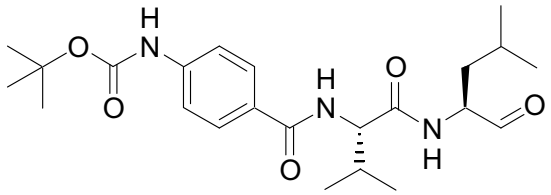

Alcohol **31c** (194 mg, 445 mmol) was oxidised using general procedure B. The crude product was purified by flash column chromatography over silica gel using ethyl acetate - petroleum ether (1:2-1:1) as eluent to give **33c** as a white solid (110 mg, 57%). R$_f$=0.45; δH (DMSO) 0.75-0.85 (12H, m, (C**H**$_3$)$_4$), 1.21-1.30 (9H, m, C(C**H**$_3$)$_3$), 1.55 (1H, m, CHCH$_2$C**H**(CH$_3$)$_2$), 2.04-2.07 (1H, m, CHC**H**(CH$_3$)$_2$), 3.19 (1H, m, C**H**CH(CH$_3$)$_2$, 4.21 (1H, t, C**H**CH(CH$_3$)$_2$), 7.50 (2H, d, 2Ar**H**), 7.59 (1H, d, N**H** Val), 7.78 (2H, d, 2Ar**H**), 7.97(1H, d, N**H**) 9.59 (1H, s, C**H**O). ^{13}C NMR (75 MHz, CDCl3) 18.8 (CH**C**H$_3$), 19.3 (CH**C**H$_3$), 21.3 (CH**C**H$_3$), 21.8 (CH**C**H$_3$), 23.0 (C**C**H$_3$), 23.4 (C**C**H$_3$), 24.0 (C**C**H$_3$), 24.1 (CHCH$_2$**C**H(CH$_3$)$_2$), 28.1 (CH**C**H(CH$_3$)$_2$), 36.3 (CH**C**H$_2$CH(CH$_3$)$_2$), 56.8 (**C**(CH$_3$)$_3$), 59.0 (**C**HCH$_2$CH(CH$_3$)$_2$), 63.8 (**C**HCH(CH$_3$)$_2$), 117.0 (**C**HCHC), 127.5 (**C**HCHC), 127.6 (CH**C**HC), 128.3 (CH**C**HC), 128.4 (CCHCH**C**), 142.3 (CHCH**C**), 152.6 (Boc**C**O), 165.8 (**C**ONH), 170.7 (**C**ONH), 201.2 (**C**HO).

N-[(S)-1-((S)-1-Formyl-3-methyl-butylcarbamoyl)-2-methyl-propyl]-nicotinamide (33d)

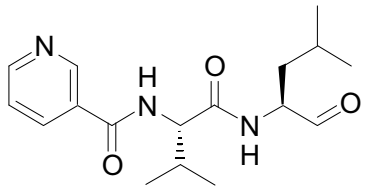

Alcohol **31d** (200mg, 0.622mmol) was oxidised using general procedure B to afford the product **33d** as a grey solid (119mg, 61%). mp 85-87°C. δH (DMSO) 0.80-0.93 (12H. m, (C**H**$_3$)$_4$), 1.30-1.45 (2H, m, CHC**H**$_2$CH(CH$_3$)$_2$), 1.63 (1H, m, CHCH$_2$C**H**(CH$_3$)$_2$), 2.10 (1H, m, CHC**H**(CH$_3$)$_2$), 4.02 (1H, m, C**H**CH(CH$_3$)$_2$), 4.35 (1H, t, C**H**CH$_2$CH(CH$_3$)$_2$), 7.51 (1H, t, Ar**H**), 8.22 (1H, d, N**H**), 8.45 (1H, d, N**H**), 8.59 (1H, d, Ar**H**), 8.70 (1H, m, Ar**H**), 8.98 (1H, s, Ar**H**), 9.40 (1H, s, C**H**O) ^{13}C NMR (75 MHz, CD$_3$OD) 18.7 (**C**H$_3$), 19.3 (**C**H$_3$), 21.3 (**C**H$_3$), 23.0 (**C**H$_3$), 24.0 (CHCH$_2$**C**H(CH$_3$)$_2$), 30.1 (CH**C**H(CH$_3$)$_2$), 39.7 (CH**C**H$_2$CH(CH$_3$)$_2$), 56.8 (**C**HCH$_2$CH(CH$_3$)$_2$), 59.2 (**C**HCH(CH$_3$)$_2$), 123.4 (CH**C**HCHC), 129.8 (CHCH**C**HC), 135.3 (CHCHCH**C**), 148.6 (CH**C**HN), 151.9 (C**C**HN), 165.3 (**C**ONH), 171.5 (**C**ONH), 201.2 (C**C**HO); (Found C, 61.23; H, 7.94; N, 12.41% $C_{17}H_{25}N_3O_3$ .0.67H_2O requires C, 61.61; H, 8.01; N, 12.68%). *m/z* (ES) $[M+(H)]^+$ 320 (50%).

5-Formyl-furan-2-carboxylicacid [1-((S)-(S)-1-formyl-3-methyl-butylcarbamoyl) -2-methyl-propyl]-amide (33e)

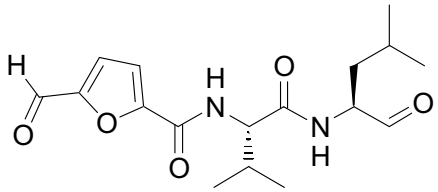

Alcohol **31e** (152mg, 0.45mmol) was oxidized using general procedure B to give **33e** as a white solid (135mg, 88%). mp 70-72 ºC; R_f = 0.28 (EtOAc / petroleum ether [1:1]);

HRMS (ES+) calcd for $C_{17}H_{25}N_3O_4$ ($M+H^+$) 336.1923 found 336.1925; ν_{max} (KBr) 1738 (CHO), 1636 (CONH); ^{1}H NMR (500 MHz, $CDCl_3$) 0.79 (3H, d, *J* 7, C**H**$_3$), 0.82 (3H, d, *J* 7, C**H**$_3$), 1.01 (3H, d, *J* 7, C**H**$_3$), 1.06 (3H, d, *J* 7, C**H**$_3$), 1.23-1.26 (1H, m, CH_2C**H**$(CH_3)_2$), 1.63-1.653 (2H, m, C**H**$_2$C**H**$(CH_3)_2$), 2.01-2.03 (1H, m, C**H**$(CH_3)_2$), 4.02-4.04 (1H, m, C**H**$CH_2CH(CH_3)_2$), 4.80 (1H, t, *J* 8, C**H**C**H**$(CH_3)_2$), 6.84-6.88 (1H, m, C**H**CH), 6.93-6.95 (1H, m, C**H**CCHO), 7.75 (1H, d, *J* 7, N**H**), 7.82 (1H, d, *J* 7, N**H**), 9.58 (1H, s, C**H**O), 9.60 (1H, s, C**H**O), 11.82 (1H, br s, N$H_{pyrrole}$); ^{13}C NMR (75 MHz, $CDCl_3$) 18.9 (**C**H_3), 19.2 (**C**H_3), 21.63 (**C**H_3), 22.8 (**C**H_3), 24.6 ($CHCH_2$**C**$H(CH_3)_2$), 30.8 (CH**C**$H(CH_3)_2$), 37.2 (CH**C**$H_2CH(CH_3)_2$), 57.5 (**C**$HCH_2CH(CH_3)_2$), 59.1 (**C**$HCH(CH_3)_2$), 111.9 (**C**HCH), 121.1, (**C**HCCHO), 132.2 (**C**CONH), 134.2 (**C**N), 160.1 (**C**ONH), 172.5 (**C**ONH), 180.6 (C**C**HO), 199.5 (CH**C**HO); *m/z* (ES) ($[M+(H)]^+$, 336 (100%); ($[M+(Na)]^+$ 358 (10%).

4-Formyl-1H-pyrrole-2-carboxylic acid [1-((S)-(S)-1-formyl-3-methyl-butyl carbamoyl)-2-methyl-propyl]-amide (33g)

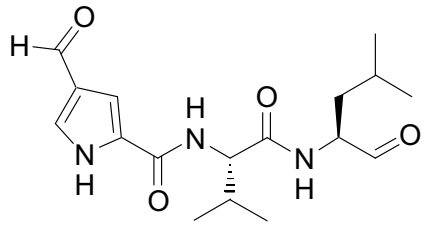

The alcohol **31g** (236.5mg, 0.372mmol) was oxidized using general procedure B to afford product **33g** as a white solid (135mg, 88%). mp 101-103^{o}C; ν_{max} (KBr) 1736 (CHO), 1643 (CONH); ^{1}H NMR (500 MHz, $(CD_3)_2SO$) 0.82 (3H, d, *J*=6.5 Hz, C**H**$_3$), 0.86 (3H, d, *J*=6.0 Hz, C**H**$_3$), 0.90 (3H, d, *J*=7.0 Hz, C**H**$_3$), 1.06 (3H, d, *J*=7.5 Hz, C**H**$_3$), 1.41-1.44 (1H, m, CH_2C**H**$(CH_3)_2$), 1.50-1.56 (1H, m, C**H**$_2$C**H**$(CH_3)_2$), 1.61-1.65 (1H, m, C**H**$_2$C**H**$(CH_3)_2$), 2.05-2.11 (1H, m, C**H**$(CH_3)_2$), 4.10-4.14 (1H, m, C**H**$CH_2CH(CH_3)_2$), 4.30 (1H, t, *J*=8.5 Hz, C**H**C**H**$(CH_3)_2$), 7.41 (1H, s, C**H**CH), 7.69 (1H, s, C**H**CCHO), 8.17 (1H, d, *J*=9.0 Hz, N**H**), 8.42 (1H, d, *J*=7.5 Hz, N**H**), 9.38 (1H, s, C**H**O), 9.72 (1H, s,

C**H**O), 12.30 (1H, br s, N*H*$_{pyrrole}$); ^{13}C NMR (75 MHz, DMSO) 18.7 (**C**H$_3$), 19.4 (**C**H$_3$), 21.6 (**C**H$_3$), 23.8 (**C**H$_3$), 24.1 (CHCH$_2$**C**H(CH$_3$)$_2$), 30.0 (CH**C**H(CH$_3$)$_2$), 36.2 (CH**C**H$_2$CH(CH$_3$)$_2$), 58.3 (**C**HCH$_2$CH(CH$_3$)$_2$), 59.8 (**C**HCH(CH$_3$)$_2$), 119.0 (**C**HCH), 126.5, (**C**HCCHO), 128.3 (**C**CONH), 130.3 (**C**N), 160.0 (**C**ONH), 171.7 (**C**ONH), 185.9 (**C**CHO) 201.2 (CH**C**HO); *m/z* (ES) [M+(H)]$^+$ 336 (100%). (Found C, 58.67; H, 7.46; N, 11.90% $C_{17}H_{25}N_3O_4$.0.67H_2O requires C, 58.77; H, 7.64; N, 12.10%). HRMS (ES+) calcd for $C_{17}H_{25}N_3O_4$ (M+H$^+$) 336.1923 found 336.1934.

1H-Indole-2-carboxylic-acid[(S)-1-((S)-1-formyl-3-methyl-butyl-carbamoyl)-2-methyl-propyl]-amide (33i)

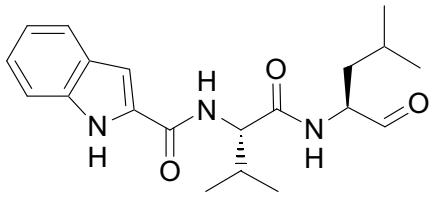

The alcohol **31i** (116mg, 323mmol) was oxidised using general procedure B to afford product **33i** as a white solid (93mg, 81%). mp 96-98^{o}C; δH (DMSO) 0.82 (3H, d, CH$_3$), 0.84 (3H, d, CH$_3$), 0.87 (3H, d,CH$_3$), 0.89 (3H, d, CH$_3$), 1.30 (2H, m, CHC**H$_2$**CH(CH$_3$)$_2$), 1.61 (1H, m, CHCH$_2$C**H**(CH$_3$)$_2$), 2.01 (1H, m, CHC**H**(CH$_3$)$_2$), 4.03 (1H, t, C**H**CH$_2$CH(CH$_3$)$_2$), 4.21 (1H, d, C**H**CH(CH$_3$)$_2$), 7.06 (1H, t, Ar**H**), 7.20 (1H, t, Ar**H**), 7.31 (1H, s, Ar**H**), 7.44(1H, d, N**H**), 7.62 (1H, d, N**H**), 7.74 (1H, d, Ar**H**), 8.26 (1H, d, Ar**H**), 11.6 (1H, s, C**H**O). ^{13}C NMR (75 MHz, DMSO) 19.5 (**C**H$_3$), 20.0 (**C**H$_3$), 22.5 (**C**H$_3$), 24.1 (**C**H$_3$), 24.9 (CH**C**H(CH$_3$)$_2$), 40.2 (CH**C**H$_2$CH(CH$_3$)$_2$), 49.4 (**C**HCH$_2$CH(CH$_3$)$_2$), 59.3 (**C**HCH(CH$_3$)$_2$), 64.5 (**C**H$_2$OH), 104.3 (NHCCH**C**H), 112.2 (NHCCHCH**C**H), 120.4 (C**C**HCH), 124.1 (NHC**C**H), 127.7 (NHC**C**), 132.0 (NH**C**C), 137.2 (NHC**C**H), 161.5 (**C**ONH), 171.3 (**C**ONH). (Found C, 65.37; H, 7.93; N, 11.24% $C_{17}H_{25}N_3O_3$ .0.5H_2O requires C, 65.55; H, 7.76; N, 11.47%). HRMS (E+S) calc for $C_{20}H_{27}N_3O_3$ ([M+H]$^+$) 358.2052 found 358.2037.

4-Amino-N-[(S)-1-((S)-1-formyl-3-methyl-butylcarbamoyl)-2-methyl-propyl]-benzamide hydrochloride salt (35)

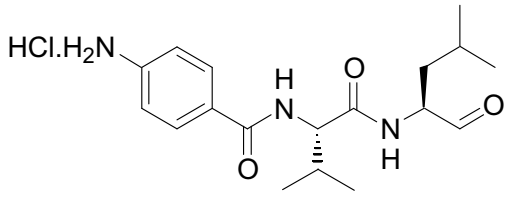

Compound **33c** (20 mg) was dissolved in HCl -dioxane (4M, 1ml) and the solution was stirred overnight. The solvent was removed on a rotary evaporator under vacuum to give product **35** as a yellow oil (17 mg, 98%). The product was used in the subsequent reaction without further purification.

3.3: Reference

[67] Schmuck, C.; Machon, U. *Chem. Eur. J.* **2005**, 11, 1109 – 1118.

[68] Aitken, S. PhD Thesis, Design, synthesis and testing of β-strand mimics as protease inhibitors. University of Canterbury. **2006**, 173.

[69] Ewan, J. T.; Robins, D. J. *Tetrahedron.* **1995,** 51, 10241-10252.

APPENDIX: ASSAY DATA

The assays were carried out by Janna Nikkel, a graduate student at Canterbury, using Lincoln University's facilities and with advice from Dr Jim Morton and his students and Dr Matthew Jones, a Post-doctoral Fellow in the group working at Canterbury.

The assay protocol used in this thesis was based on the protocol of Thompson et al[1] and makes use of casein, a water soluble protein, labeled with the fluorophore 4,4-difluoro-5,7-dimethyl-4-bora-3a,4a-diaza-s-indacene-3-propanoic acid (BODIPY).

Compounds **33a-k** were assayed against m-calpain and their inhibition constant (IC_{50}) value determined.

The solution of m-calpain was produced by Dr Jim Morton.

The assays were performed in 96-well black *Whatman* plates.

Two blank control assays were utilized;

Calcium blank: 100 μL of 100 mM calcium chloride,

Addition of BODIPY-casein to this blank results in no reaction and thereby provides the base line for the fluorometer.

EDTA blank: 25 μL of 10 mM EDTA solution diluted with 25 μL distilled water and 50 μL of the enzyme in sample buffer (20 mM TRIS-HCl, pH 7.5 containing 1 mM EDTA, 1 mM EGTA, and 2 mM mM TRIS-HCl, pH 7.5 containing 1 mM EDTA, 1 mM EGTA, and 2 mM dithiothreitol)

Addition of BODIPY-casein to this blank results in no reaction since the calcium ions are bound to the EDTA, thus the m-calpain cannot be activated. This confirms the base line in the fluorometer.

The assay:

Calpain activity control assay: 50 µL m-calpain in sample buffer (20 mM TRIS-HCl, pH 7.5 containing 1 mM EDTA, 1 mM EGTA, and 2 mM dithiothreitol) diluted with 50 µL distilled water.

The inhibitor assay: 50 µL m-calpain and 50 µL of inhibitor (of known concentration) diluted in distilled water.

The reaction of m-calpain and BODIPY-casein in both the presence and absence of inhibitor was initiated by the addition 100 µL of BODIPY-casein substrate solution to each well at 25 °C. The progress of each reaction was followed for 10 min in an automated BMG Fluostar fluorometer with excitation of 485 nm and measuring emission of 530 nm.

The percentage inhibition was determined as the percentage of the m-calpain activity with inhibitor present compared with the activity of the control m-calpain activity assay.

Assays were performed in triplicate with serial dilutions of inhibitor concentrations from 50 µM to 50 nM.

Concentrated BODIPY-casein was supplied by Lincoln University. A fresh batch of the diluted BODIPY-casein substrate solution was prepared for each assay. The BODIPY

casein substrate solution comprises: digestion buffer (500 µL) (prepared from 2ml 100 mM tris(hydroxymethyl)methylamine and 2 ml 10 mM sodium azide, adjusted to a pH 7.8 by the addition of 10 mM sodium hydroxide and the solution diluted to a volume of 10 ml with water) deionized water (8440 µL), 100 mM $CaCl_2$ (1000 µL), BODIPY-casein (50 µL) and β-mercaptoethanol (10 µL).

The stock solutions of inhibitor were prepared as 1 mM solutions in DMSO. Further dilutions by the addition of distilled water gave the range of concentrations: 50, 10, 2, 0.4, 0.2, 0.1 and 0.05 µM for inhibition assay.

The percent inhibition of m-calpain for each compound was calculated based on the average change in fluorescence[70]; the assay data obtained was plotted on a graph as percentage inhibition versus the log of inhibitor concentration. IC_{50} was then determined as shown in **Figure 30**.

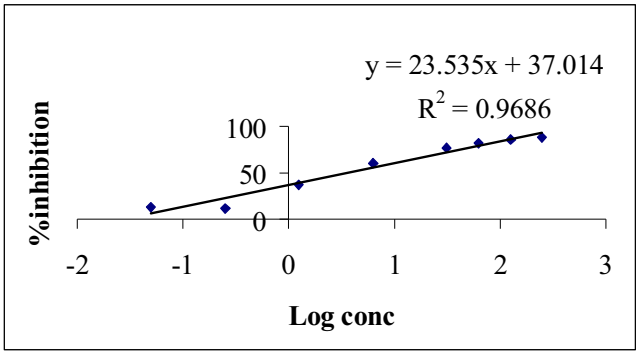

conc	log(conc)	% inhib
250	2.4	88.8
125	2.1	86.0
62.5	1.8	81.4
31.25	1.5	76.8
6.25	0.8	60.1
1.25	0.1	37.5
0.25	-0.6	12.2
0.05	-1.3	12.9

Figure 30: Linear inhibition date for **33b.** The percentage inhibition was plotted against the log value of inhibitor concentration. The linear best fit was obtained and the IC_{50} value was calculated using the equation for the line of best fit. The corresponding log value was converted back to units of concentration (3.56 µM).

References for Appendix

[70] Thompson, V. F.; Saldana, S.; Cong, J.; Goll, D. E. *Analytical Biochemistry.* **2000**, *279*, 170-178.